Project title:	Modelling Light Leaf Spot (*Pyrenopeziza brassicae*) on Oilseed Rape (*Brassica napus*) and Vegetable Brassica (*Brassica oleracea*).
Project number:	CP179
Project leader:	Thomas Crocker, Newcastle University
Report:	Final report, January 2023
Previous report:	Annual, May 2021
Key staff:	Roy Sanderson, Newcastle University
Location of project:	Fera Science Ltd
Industry Representative:	Femke van den Berg, Fera Science Ltd Judith Turner, Fera Science Ltd
Date project commenced:	23 September 2018

DISCLAIMER

While the Agriculture and Horticulture Development Board seeks to ensure that the information contained within this document is accurate at the time of printing, no warranty is given in respect thereof and, to the maximum extent permitted by law the Agriculture and Horticulture Development Board accepts no liability for loss, damage or injury howsoever caused (including that caused by negligence) or suffered directly or indirectly in relation to information and opinions contained in or omitted from this document.

The results and conclusions in this report are based on an investigation conducted over a one-year period. The conditions under which the experiments were carried out and the results have been reported in detail and with accuracy. However, because of the biological nature of the work it must be borne in mind that different circumstances and conditions could produce different results. Therefore, care must be taken with interpretation of the results, especially if they are used as the basis for commercial product recommendations.

AUTHENTICATION

We declare that this work was done under our supervision according to the procedures described herein and that the report represents a true and accurate record of the results obtained.

Thomas Crocker

PhD student

Newcastle University

Signature ..... T. Crocker ..... Date .....26th January 2023.....

Roy Sanderson

Senior Lecturer in Biological Modelling

Newcastle University

Signature .... Date .....23rd January 2023.....

Femke van den Berg

Senior Scientist in Mathematical Modelling in Plant/Crop Health

Fera Science Ltd

Signature ..... Date .....19/01/2023.....

Report authorised by:

[Name]

[Position]

[Organisation]

Signature ..... Date .....

CONTENTS

GROWER SUMMARY

Headline

A new infection model for light leaf spot on winter oilseed rape (WOSR) and vegetable brassica (VB) was developed to improve disease forecasting efforts in both host types. The model was developed from a mixture of laboratory, glasshouse and field survey experiments to simulate key components of the pathogen lifecycle.

Background

Light leaf spot (*Pyrenopeziza brassicae*) is an important fungal pathogen that affects all commercially cultivated *Brassica* crops. WOSR and specific varieties of VB with long growing seasons such as Brussel sprouts (*B. oleracea* var. *gemmifera*) and storage cabbage (*B. oleracea* var. *capita*) are particularly vulnerable. The pathogen is regarded as one of the most damaging diseases of WOSR – resulting in up to 30% yield losses in badly affected crops, and in VB yield losses have been reported to be as high as 10% per annum.

P. brassicae is capable of multiple cycles of infection and sporulation each year. Primary infections are caused by windborne ascospore released from contaminated necrotic tissue such as dropped leaves and debris left over from harvested crops. Ascospore infections are thought to occur at low frequency, producing a random distribution of infected plants early in the growing season. From these initial foci the disease spreads to neighbouring plants via splash-dispersed conidia which are released from living host tissue; causing the distribution of infections to become patchy as the growing season progresses. Initially, infections caused by ascospore or conidia are asymptomatic, the disease cannot usually be detected during this latent period by visual assessment before conidia production begins. Both ascospore and conidia are released throughout the growing season allowing the disease to build up rapidly in response to favourable environmental conditions. Together these characteristics make it difficult to visually assess disease severity in WOSR or VB crops which hinders effective disease control.

Light leaf spot is characterised by white masses of conidia that form on latently infected tissue. Conidia production occurs during high humidity and are splashed off the leaf by rain. As the disease develops more permanent necrotic damage becomes visible, taking the form of ‘thumb-print’ lesions in VB and mealy regions of chlorosis and necrosis in WOSR. The latent period of the pathogen has been determined by laboratory experiments to be between 10 and 30 days. In WOSR visible symptoms are rarely seen before spring leading early researchers to conclude that primary infection by ascospore must occur on WOSR around November and

that the pathogen must build up within a crop by production of conidia over winter to reach detectable levels by spring. However, more recent research has shown that *P. brassicae* ascospore are present above WOSR crops throughout summer and autumn thus infection could theoretically occur earlier in the WOSR growing season. The environmental factors that affect light leaf spot infection and the length of the latent period are unclear. VB are typically planted between late spring and early summer and disease symptoms can become visible from August onwards.

As the growing seasons between WOSR and VB overlap there is the potential for a 'green bridge' to occur, allowing disease epidemics from one crop to move into the other, and between growing seasons. WOSR is the most widely cultivated brassica in the UK, being the third most widely grown arable crop after wheat and barley. It is combinable and tolerant to a wide range of soil types and environmental conditions making it useful as a break crop in cereal rotations. VB are high value horticultural crops with intense manual labour requirements and production is concentrated around small regions with fertile soils plus the infrastructure to support crop establishment from seedlings, through to harvesting, and onwards to supermarket supply chains. Their relatively high value means that routine fungicide applications in VB are almost always economically viable whereas in WOSR growers are more likely to adjust inputs in response to perceived risks. Given the larger areas cultivated for WOSR, it is likely that the main risks are transmission from WOSR to VB, potentially exacerbated as the mechanical harvest of WOSR can send large amounts of potentially infected debris into the air where it can be carried long distances by the wind

Suppression of light leaf spot is achieved by applying fungicides, planting resistant varieties and implementing cultural controls such as crop rotation, later sowing dates and cultivation after harvest to bury contaminated debris. These control measures may conflict with efforts to curb fungicide usage and no-tillage regimes designed to improve soil structure. Given the increased prevalence of severe light leaf spot epidemics in the past 20 years they are widely held to be insufficient by growers. To help growers manage the disease, AHDB releases a light leaf spot forecast that predicts the proportion of WOSR fields likely to experience 'severe' epidemics (i.e. > 20% of plants infected) by spring based on regional summer temperatures, winter rainfall and some field-level variables e.g. sowing date and the crop AHDB resistance rating. The forecasting system can help WOSR growers decide whether to apply fungicides in autumn and spring but provides only limited field level information because its predictions are averaged over large regions and released only twice yearly. In recent years field-level weather data has become more accessible and remote sensing technologies can now provide detailed maps of the annual distribution of WOSR fields. There is a need for improved disease modelling that can make use of these new field-level data inputs to better inform WOSR and

VB growers so that they can use fungicides more effectively and achieve acceptable light leaf spot control.

Summary

A primary aim of this research was to develop mechanistic models of the light leaf spot disease cycle, through understanding processes from spore germination through to the field-scale. Specific objectives were to

a) quantify spore germination and germtube growth in artificial media across a range of temperatures. Two models for germination and germtube extension were developed.

b) quantify spore germination and germtube growth on WOSR and VB leaf disks. This was done on a subset of temperatures identified from the artificial media experiments, and likely to occur in the field. Both susceptible and partially resistant strains of WOSR and VB were investigated, and the two models from a) updated accordingly.

c) determine infection in WOSR and VB plants. Glasshouse-grown plants were infected with *P. brassicae* under different leaf wetness durations and temperatures, to reflect a range of scenarios likely to occur in the field. This allowed the effects of infection severity to be distinguished from the effects of temperature post-infection. The infection model developed from this component of the research can use time-series data, for example derived from meteorological temperature and rainfall, as inputs.

d) model light leaf spot under field conditions. Pathogen development in WOSR field plots was assessed relative to meteorological conditions, aerial spore data and landscape scale distribution of WOSR fields.

The research presented provided a thorough understanding of aspects of these four components, but also highlighted gaps in knowledge where additional studies are required. An outstanding challenge is to integrate across scales, particularly from laboratory and glasshouse experiments to the field conditions.

The initial experiments were designed to understand key environmental factors that affected *P. brassicae* spore germination, and germtube growth rates, first in artificial media, second on detached leaf disks, and finally glasshouse plants. It was assumed that direct observations of the pathogen would be more informative than observations of light leaf spot symptoms, given the pathogen's latent period before symptoms are visible. It was anticipated that spore germination and germtube growth rate might vary between host types because of physical and molecular differences in the leaf surfaces, and potentially differences in disease resistance. The need for a minimum germtube length before infection was also considered. Variation in leaf level resistance mechanisms in *B.*

oleracea and *B. napus* might have important implications for modelling infection in vegetable brassica and WOSR crops in the field.

The research indicated that the characteristics of the leaf surface (as defined by the host type) in practice had little effect on germination and germtube tube extension of *P. brassicae* conidia compared to spores that were allowed to develop in artificial media. Their early development was in all cases principally influenced by the temperature. Furthermore, the threshold germtube length required for infection of *B. napus* was very close to zero, suggesting that infection can occur following germination irrespective of germtube length. Whilst germination is possible at temperatures above 20 °C, this is much higher than optimum infection temperatures (Gilles et al., 2001), and rarely occurs in the UK with periods of sustained leaf wetness under field conditions. Thus, a simpler infection model that predicted infection severity by fitting a restricted exponential equation to the thermal time accumulated during a period of leaf wetness was implemented. This indicated that infection first becomes possible after approximately 90 °C hours and that the by 573 °C hours infection severity reaches 95% of its maximum value. Under field conditions a simple 90 °C hour threshold in combination with a 2 mm per hour rain intensity threshold is enough to distinguish leaf wetness periods that are suitable for infection from those that are too short, too cold or lack sufficient rainfall for splash dispersal of conidia.

These models required relatively simple weather data inputs, therefore in-field weather stations or short-term weather forecasts could be used to make field-level predictions. When the infection model was run at a series of WOSR field sites it was found that the number of infection events detected from September to April was significantly correlated with disease incidence in spring with the number of infection events explaining approximately 50% of the variation in incidence. At all field sites infection events were evenly dispersed throughout the growing season, suggesting that the environment can potentially be suitable for light leaf spot infection throughout the year.

Financial Benefits

A significant relationship was discovered between the number of predicted infection events detected during an WOSR growing season and light leaf spot disease incidence in spring. This will have direct applications to existing disease forecasting systems by providing an additional field-level variable that can be used to predict the severity of the light leaf spot epidemic. The infection models have been developed from a fundamental analysis of the mechanisms behind spore germination in relation to weather and thus it is likely that its

predictions will be relatively resilient to short-term future changes to weather patterns or farming practices. Therefore, this model could be integrated into the AHDB light leaf spot forecast on WOSR to enhance its capabilities, or alternatively it could form the basis of a new dynamic forecasting system for light leaf spot on both WOSR and VB.

Action Points

- Further work should focus on the implementation of the models developed during this project into forecasting / decision support systems that can be used by growers to make crop management decisions.
- Given that infection events and ascospore release were predicted to occur throughout the year it is likely that light leaf spot infections occur earlier in the growing season than previously thought. Growers may benefit by switching to earlier fungicide applications if the conditions at the start of the WOSR growing season have been favourable for the pathogen. Further work is however required to investigate how such alterations would impact the existing WOSR spray program targeting all WOSR pathogens, in particular, stem canker and alternaria.
- Additional field research should be conducted with untreated vegetable brassica plots to test if the same relationship between infection events and disease incidence also holds true for *B. oleracea* crops under growing conditions typical of a commercial enterprise.
- New research into the distribution of *P. brassicae* ascospore should be considered using *B. napus* field plots established in more remote locations further from potential sources of infection.

SCIENCE SECTION

Introduction

Pyrenopeziza brassicae is a polycyclic ascomycete that causes light leaf spot in a broad range of brassica hosts (Karolewski 2010; Rawlinson et al. 1978). Historically, light leaf spot has been the main disease threat in Scotland and the north-western regions of England to vegetable brassica crops with long growing seasons like Brussels sprouts and cabbage. However, since the first major epidemic on WOSR in 1974 (Rawlinson et al. 1978), severe outbreaks have been damaging crops in previously unaffected southern and eastern regions on a semi-regular basis. There were major epidemics in 1989, 1995, and 2001 with especially severe epidemics in the northern and western regions (Fig. 1). Since 2008 severe epidemics have tended to occur annually, even in southern regions that were previously less affected. In VB there is no widely available disease monitoring data for light leaf spot, but growers have reported that the disease is becoming an increasing problem in large centres of VB production, for example around Lincolnshire (Sharp 2022; Anon. 2019), a region of the UK that has not been at high risk historically.

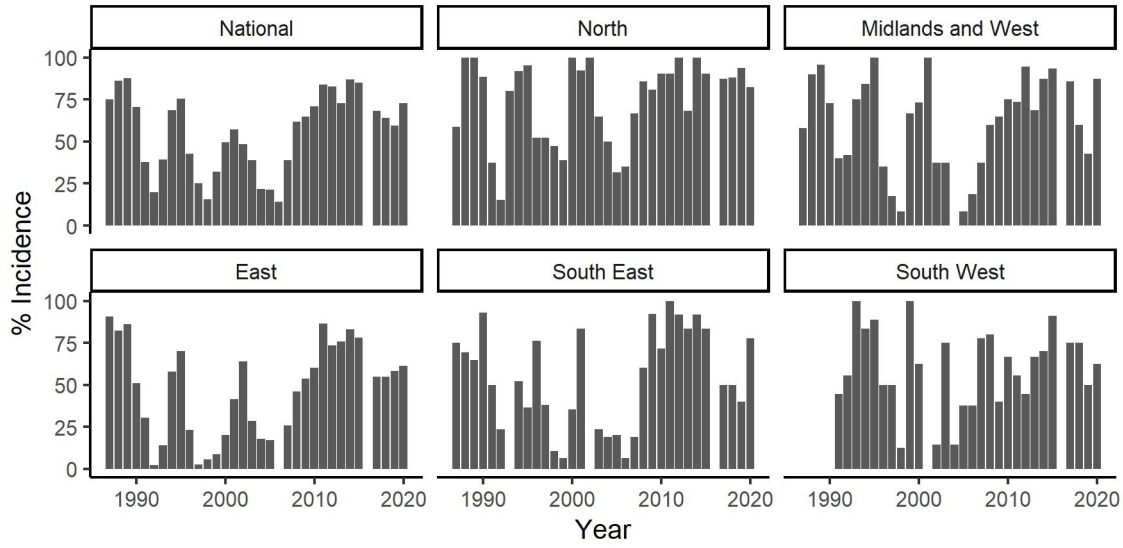

Figure 1 National and regional light leaf spot incidence recorded by the DEFRA oilseed rape spring survey by visually assessing 30 plants from approximately 100 oilseed rape fields sampled each year from across England and Wales

P. brassicae epidemics are initiated in healthy crops by airborne ascospores (Evans et al. 2003). Ascospores are released from apothecia that develop on contaminated debris dropped from the current crop or left over from the previous growing season (McCartney and Lacey 1983; Gilles et al. 2000b; Boys et al. 2007). They can be dispersed by wind over several kilometres enabling long-distance transmission between fields without any anthropogenic or

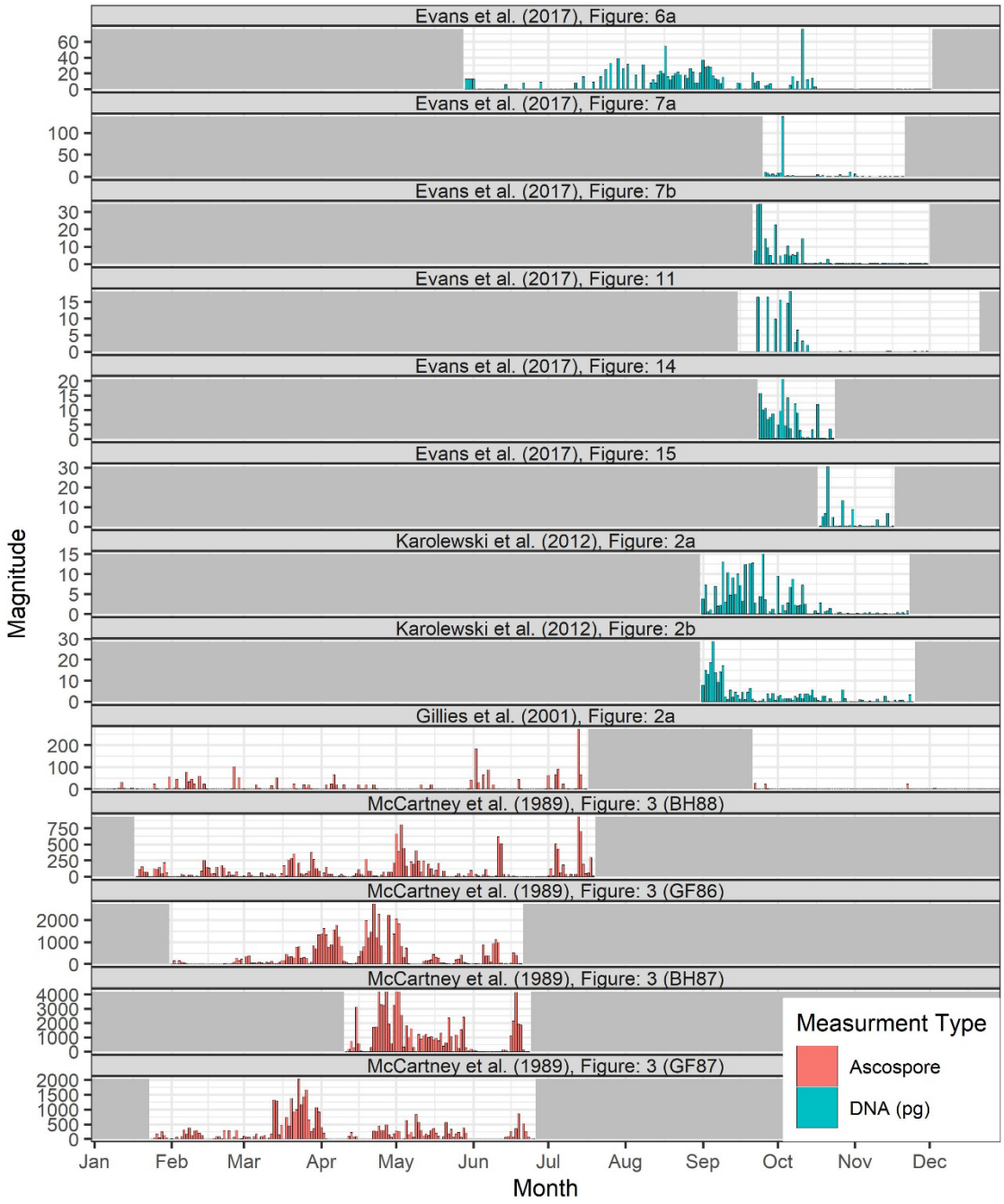

Figure 2. Published daily airborne P. brassicae concentrations captured using 7-day rotary Burkard spore traps published by various monitoring projects from across the UK.

biological vectors (McCartney et al. 1986). Airborne *P. brassicae* inoculum has been monitored over the growing season using daily spore traps plus light microscopy (McCartney and Lacey 1983; Gilles et al. 2001c) or more recently, molecular techniques such as qPCR (Evans et al. 2017; Karolewski et al. 2012). Whilst the start and end dates of each monitoring effort have varied, significant concentrations of airborne inoculum have been detected from early November to late February above naturally infected WOSR across the UK (Fig. 2).

Although these surveys indicate that *B. napus* and *B. oleracea* may potentially be exposed to ascospores throughout the year (Fig. 2) visible symptoms are rarely seen in WOSR before

January (Fitt et al. 1998a; Karolewski et al. 2006*)* and not in VB until after August (Behrends et al. 2020), three to four months after their respective sowing / planting dates. It has been suggested that environmental conditions suitable for infection may be common at all times of year which, if true, would imply that infection by airborne ascospores in the field is a frequent occurrence (Evans et al. 2017). The latent period in WOSR was reported by (Figueroa et al. 1995b) to be in the region of 150-250 degree-days and by (Gilles et al. 2000a) to take twenty to thirty days at temperatures between 5 and 20°C. However, Figueroa et al. (1995b) also recorded the time between infection and disease development to take up to 40 days under field conditions. If the first *P. brassicae* infections occur in *B. napus* after emergence (September-October) this should cause the first visible symptoms to develop between November and December, whilst, infections that occur soon after vegetable brassica seedlings are planted out (April/May) should become visible between June and July (Fig. 3). The apparent mismatch between the expected and observed occurrence of light leaf spot symptoms highlights a gap the current understanding of the *P. brassicae* disease cycle that might be explained either by a lack of suitable environmental conditions for infection or *P. brassicae's* latent period being longer than previously assumed.

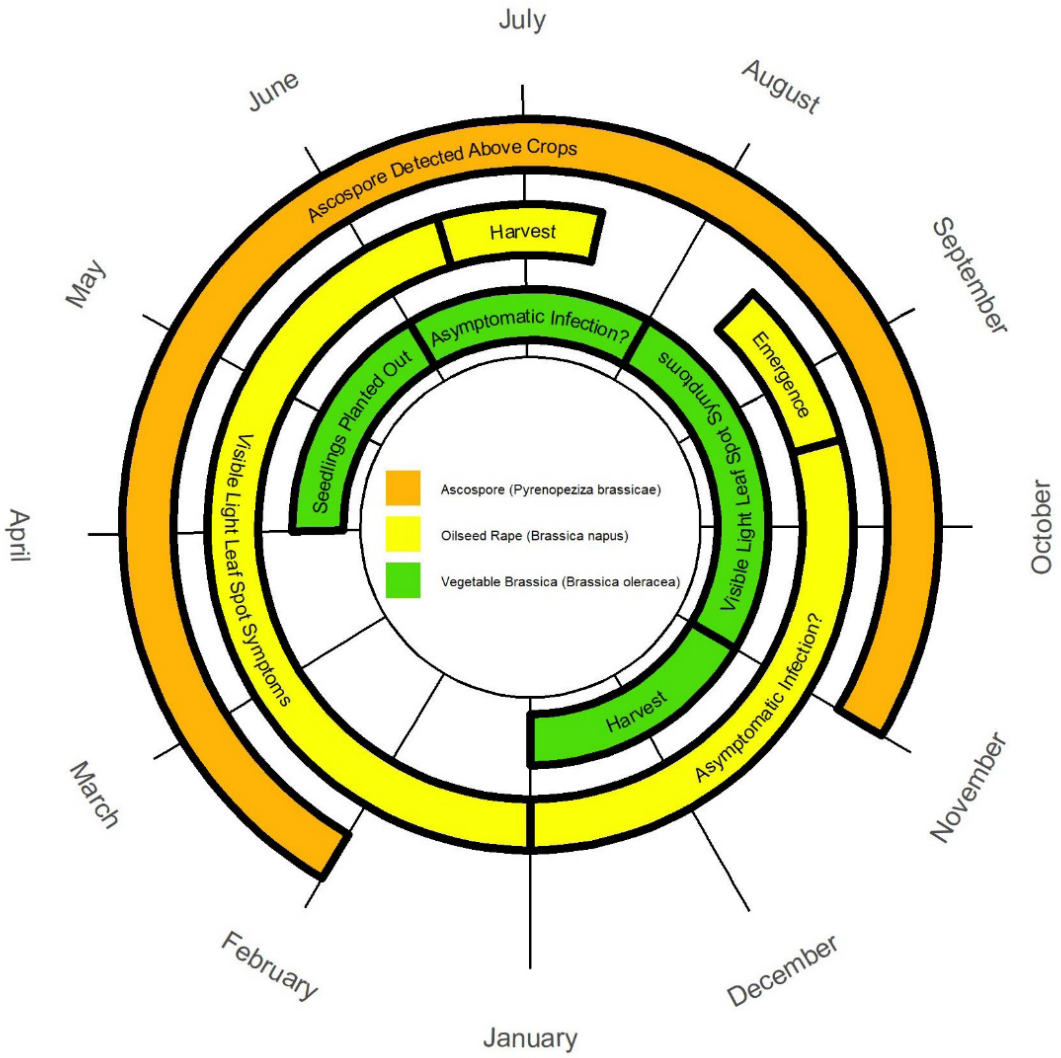

Figure 3. Annual light leaf spot epidemic on WOSR (yellow) and late-harvested VB (green) showing the establishment of new crops, the first observation of light leaf spot symptoms and approximate harvest times. Orange bar shows reported periods when airborne P. brassicae ascospores have been detected above WOSR (Evans et al. 2017; McCartney and Lacey 1989; Karolewski et al. 2012; Gilles et al. 2001c)

Several models and forecasting systems have been developed for light leaf spot based on the current understanding of the disease cycle and visual observations of the disease in the field. First, mechanistic models of disease development based on controlled environment experiments that linked temperature and leaf wetness duration to ascospore release, infection and the length of the latent period (Figueroa et al. 1995b; Gilles et al. 2000a; Gilles et al. 2001a; Gilles et al. 2001b). Second, compartment models to simulate healthy, infected, infective and dead leaves of WOSR plants exposed to ambient environmental conditions (Papastamati et al. 2002). Third, empirical forecasting systems that link long term weather variables and regional measures of disease intensity at the end of the previous growing season to regional, field level incidence in spring using survey data to fit parameters (Welham

et al. 2004). Of the three techniques only the empirical forecasting system has been maintained and made available to growers on a regular basis by AHDB (AHDB 2022).

The light leaf spot disease cycle begins when wind-borne ascospores or splash-dispersed, asexual conidia are deposited onto the leaves, stems, petals or pods of susceptible brassica hosts (Boys et al. 2007) (Fig. 4). Once deposited on the leaf surface *P. brassicae* spores can remain dormant until conditions are suitable for germination (Maddock and Ingram 1981). Spore germination requires sufficient time at appropriate temperatures in the presence of free water (Figueroa et al. 1995b; Karolewski et al. 2004). The fist visible sign of germination is the development of a single germtube with a diameter of approximately 1 µm that emerges close to the tip in both spore types. Germtubes develop along the outer surface of the leaf avoiding stomata until they can penetrate the cuticle directly (Davies et al. 2000). The germtube swells slightly at the point of entry but no appresorium is formed, instead it is thought that entry is achieved by enzymatic degradation of the cuticle mediated by an extracellular cutinase (Li et al. 2003). Both spore types germinate between 4 and 24 ^{o}C but germination may be possible beyond this range (Figueroa et al. 1995b; Karolewski et al. 2004). There is some evidence that the germtube extension rate in ascospores is faster than that of conidia (Karolewski et al. 2004) and fewer ascospores are required to produce the same level of disease severity in infected WOSR under controlled environmental conditions (Karolewski et al. 2002).

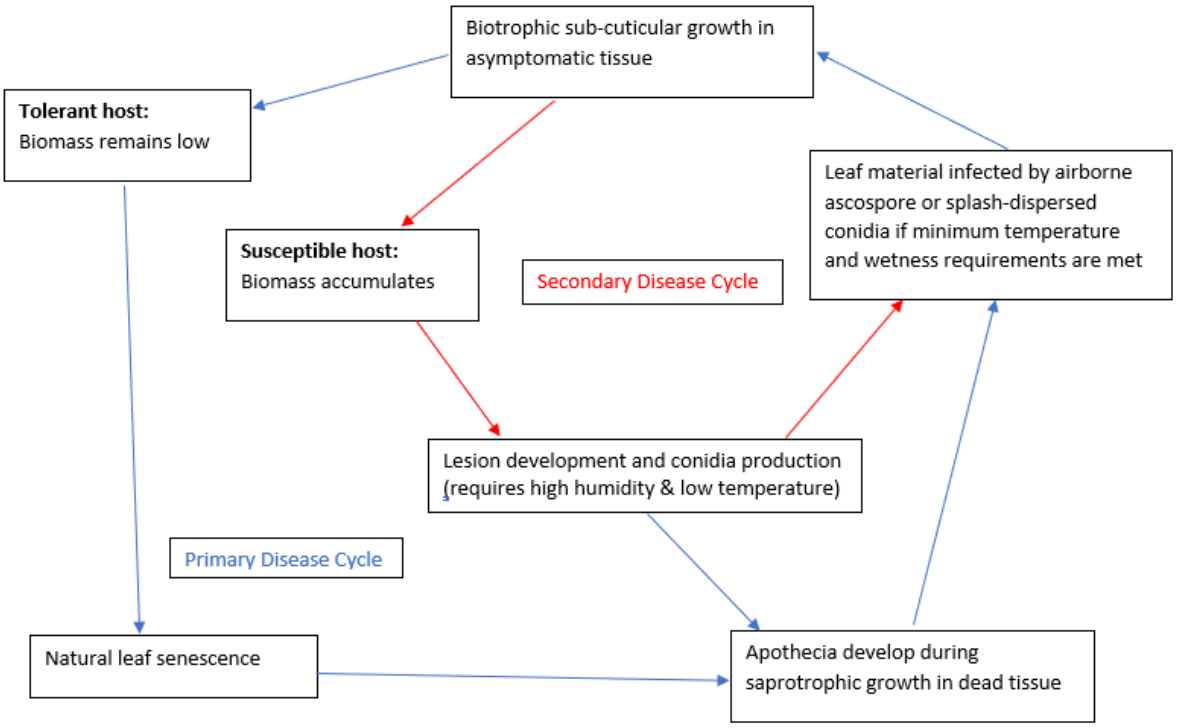

Figure 4. The disease cycle of the *P. brassicae* - *Brassica* pathosystem

Once *P. brassicae* has penetrated the cuticle it develops slowly within the sub-cuticular space (Li et al. 2003). The germtube differentiates into branching hyphae which develop along the surface of the epidermal cells beneath the cuticle, preferentially following leaf veins which are thought to provide better access to nutrients (Karandeni Dewage et al. 2022). After establishment within the sub-cuticular space the pathogen no longer requires free water on the leaf surface for survival and the pace of its development is principally controlled by temperature (Gilles et al. 2001b). Initially *P. brassicae* enters a long biotrophic phase during which it builds an extracellular hyphal network close to the leaf surface with relatively few structures that penetrate deeper within the leaf (Rawlinson et al. 1978). This behaviour might help it to avoid detection by host defence mechanisms which can lead to a black flecking response soon after infection in host types that possess major-gene mediated resistance (Boys et al. 2012; Karolewski et al. 2010).

The first visual symptoms in susceptible hosts are caused by interactions between the pathogen and the host's growth regulatory system (Ashby 1997). Infected leaves typically possess elongated petioles and excessive leaf curling/deformation (Ashby 2000) which can be indicative of infection in the absence of other symptoms (Karandeni Dewage et al. 2021). Twenty to thirty days after infection the biotrophic phase ends and the first visible signs of damage appear. White masses of conidia are produced by acervuli that erupt from beneath the cuticle (Rawlinson et al. 1978). In *B. oleracea* these tend to form in concentric rings alongside a pattern of necrotic flecking typically described as a 'thumbprint'. In *B. napus*

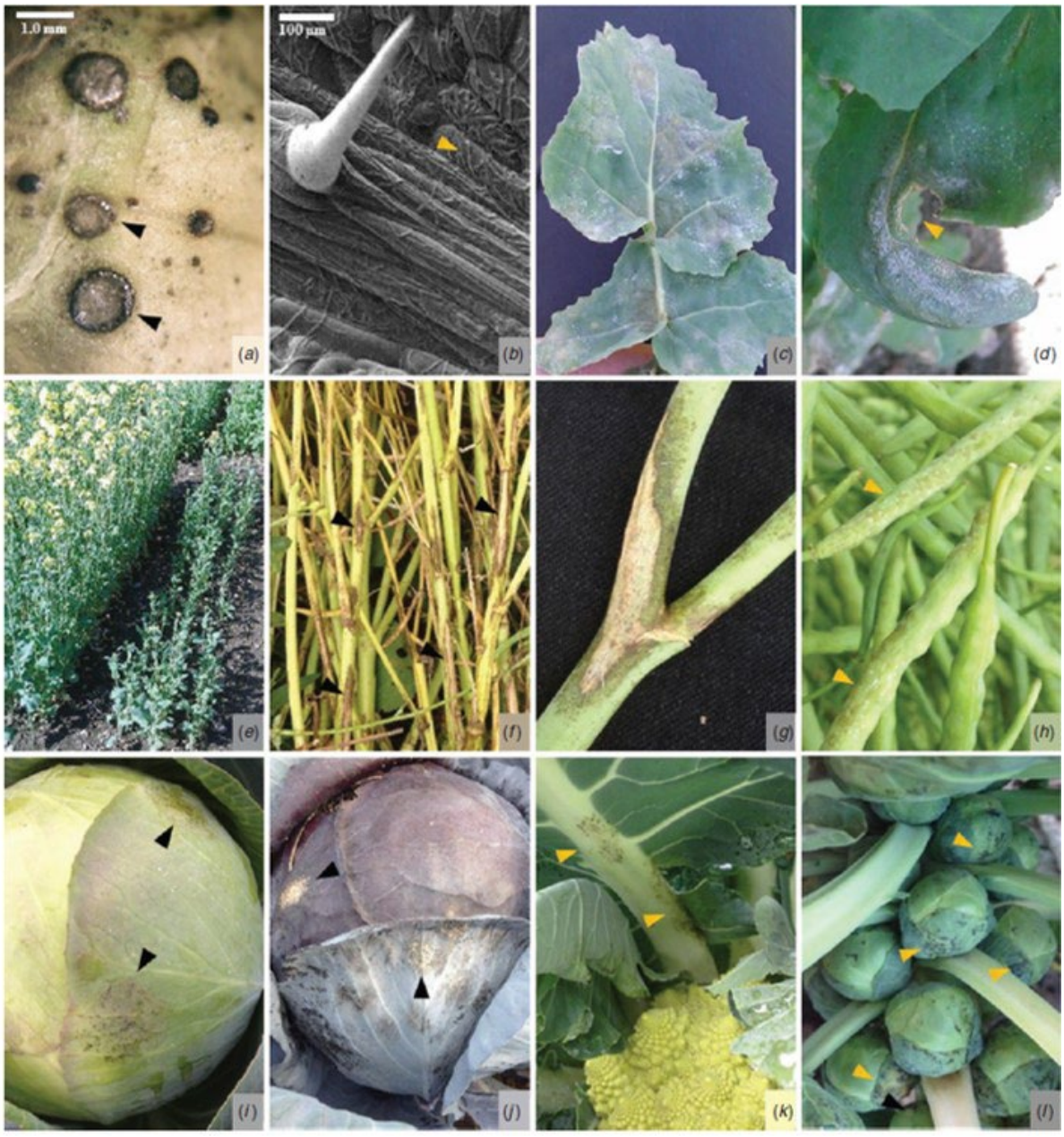

Figure 5. (a) mature apothecia on WOSR (b) scanning electron microscopy image of *P. brassicae* hyphal network developing within subcuticular space (c & d) white conidia masses and 'mealy' necrotic lesions on WOSR (e) stunting in artificially inoculated WOSR plants (right) next to healthy plants (left) (f & g) necrotic lesions on WOSR stems (h) conidia masses and black flecking on WOSR pods (I & j) 'thumbprint' lesions on cabbage heads (k & f) black flecking and thumbprint lesions on the stems and buttons of Brussel sprouts.

sporulation tends to be more widespread and the necrotic flecking is less well defined (Fig. 5). Green islands of apparently healthy tissue can become visible at sites of infection as non-infected parts of the leaf discolour due to stress responses or chlorosis (Ashby 2000). In severe infections whole leaves can be consumed (Fitt et al. 1998a).

The conidia masses are readily dispersed in water allowing them to be spread by rain splash to neighbouring plants (Evans et al. 2003) and up the canopy to new leaves and pods (Pielaat

et al. 2002). Meanwhile, apothecia begin to develop in necrotic tissue and dropped leaves. Apothecia maturation on infected material requires moisture and is known to be temperature dependant (Gilles et al. 2001a). The mechanism for the release of ascospores into the air is not completely understood but monitoring data (McCartney and Lacey 1983; Evans et al. 2017; McCartney et al. 1986; Gilles et al. 2001c) and experiments involving ascospore production (Karolewski et al. 2002; Figueroa et al. 1995b) suggest that release is stimulated by the drying of wet material containing mature apothecia (e.g. in dry weather after morning dew or rainfall)

Disease forecasting of light leaf spot has proved challenging, despite many decades of research into the pathogen. Models that predict infection and latency in relation to temperature and leaf wetness duration (Gilles et al. 2001b) have been shown to be somewhat effective in outdoor pot experiments under high disease pressure (Papastamati et al. 2002). However, attempts to extend these models to incorporate weather data, airborne ascospore concentrations and disease observations collected from the field have been unsuccessful (Evans et al. 2017). One problem is that challenges associated with diagnosis (Fitt et al. 1998a) and variable rates of disease development post-infection (Boys et al. 2012; Karandeni Dewage et al. 2022) have made it difficult to detect infection events early in the season.

Researchers studying other pathogens with long latent periods have overcome this problem by direct measurement of potential infection events, instead of relying on symptom development (de Vallavieille et al. 1995). A similar approach might be useful for *P. brassicae*. This would have additional benefits, in that a model based on pathogen biology could be more easily adapted to different host types/species with different levels of resistance, and the development of a new model presents an opportunity to use hourly weather inputs which may be more realistic given the short leaf wetness times required produce symptoms (Gilles et al. 2000a). An effective infection model based on simple meteorological inputs could be supplied with hourly data from 1 km gridded weather products such as the UK Meteorological Office (UKMO) 'HadUK-Grid' (UKMO 2022). This would allow field level infection risk to be estimated across the UK based on standardized local weather data, a method that has proved effective for other plant pathogens (Thayer et al. 2006; Kang et al. 2010).

This report documents the development of a related series of models that describe the light leaf spot disease cycle from germination of spores on the leaf surface, infection and disease development, through to dispersion of ascospores and conidia and spatio-temporal analysis of light leaf spot in untreated WOSR field plots. The models were based on experiments carried out in artificial media and detached leaves from *B. oleracea* and *B. napus*, controlled environment using whole plants of both host types, data collected from the field as well as re-analysis of data previously published. The aim of these models was to improve upon the

current understanding of the light leaf spot disease cycle especially the timing of infection at the start of the WOSR growing season. This will help to identify methods that can be used to predict the severity of light leaf spot epidemic at the field level to enable growers to better manage the disease.

Materials and methods

Preparation of Conidia Suspension

Eight single spore isolates of *P. brassicae* originally sampled from oilseed rape fields from across the UK during the 2017-2018 growing season as part of the Defra Pest and Disease Survey and three additional samples isolated from two trial plots at Fera Science Ltd. and a site near Scunthorpe, North Lincolnshire as part of the SMART monitoring project of the Centre of Crop Health and Protection (CHAP) (Table: 1) were grown on malt-extract agar for several weeks. When the plates were completely covered with mycelium, conidia suspensions were made by pouring 10 ml of sterile distilled water over the plates and rubbing vigorously with a sterile plastic spreader. The raw suspensions were poured off, separated into aliquots and stored at -20°C until needed.

Table 1 The id, region of origin, host of origin and year of isolation of the *P. brassicae* isolates used to make spore suspensions

Isolate ID	Region	Host Species	Harvest Year
Pb010	West Midlands	*B. napus*	2017
P14	Yorkshire	*B. napus*	2019
P17	Yorkshire	*B. napus*	2019
P18	Yorkshire	*B. napus*	2019
Pb035	East	*B. napus*	2017
Pb041	East	*B. napus*	2017
Pb080	East Midlands	*B. napus*	2017
Pb081	Yorkshire	*B. napus*	2017
Pb088	Yorkshire	*B. napus*	2017
Pb0126	North West	*B. napus*	2018
Pb093	North East	*B. napus*	2018

A single purified mixture of all conidia suspensions was made by mixing 100 µl of each raw suspension into a single Eppendorf tube then spinning the suspension at 4000G for 2 minutes in a Fisher Scientific accuSpin Micro 17 centrifuge. The supernatant containing the malt extract solution was poured off and the pellet re-suspended in 1 ml of molecular grade sterile distilled water by vortexing using a Scientific Industries (SITM) vortex genie 2. This process was repeated three times to ensure all traces of the growth media were removed. The purified suspension was split into ten aliquots and stored at -20°C until needed.

Slide Preparation

Artificial media experiment

Slides were prepared in advance of the experiment and stored in a freezer at -20°C until needed. An aliquot of the purified conidial suspension was chosen at random and its concentration was measured using a haemocytometer. A 200 µl suspension containing 2.6 x 10^6 spores ml^{-1} was prepared by diluting a small volume of the purified conidia suspension in sterile distilled water. The concentration of the new suspension was checked again using a haemocytometer and adjusted as necessary by adding more of the concentrated conidia suspension or more water.

Hanging drop slides were created by first laying a coverslip on a clean area of lab bench. An inoculation loop was used to spread a thin layer of petroleum jelly around the edge of the coverslip taking care not to mark the centre. A 1.6 µl suspension of 2.6 x 10^6 spores ml^{-1} was pipetted onto the centre of the coverslip then a fresh tip was used to pipette 0.8 µl of 2\% malt extract solution into the first drop and mix the two fluids together producing a drop containing approximately 0.6% malt extract and 1.56 x 10^6 spores ml^{-1}. A cavity slide was lowered, cavity side down, onto the coverslip creating a hanging drop, the petroleum jelly held the slide and coverslip together and formed a watertight seal around the drop. Once assembled each slide was immediately placed into a 9 cm petri dish on a bed of moist paper towels and moved to a freezer at -5^{o}C.

Leaf disk experiment

The same methods as described earlier for the artificial media were used to create conidia spore suspensions at 10^6 spores ml^{-1}. As the experiments were undertaken using slightly different conidial suspensions, a small number of hanging drop slide preparations were also created for comparison purposes. These are referred to as the ‘2020 conidia’ from the artificial media experiment, and ‘2021 conidia’ for the leaf disk experiments from hereon.

Three host plants were grown: a widely-grown Brussel sprouts cultivar (*Brassica. oleracia var. gemmifer* cul. Dagan), a susceptible OSR variety with an AHDB light leaf spot resistance rating of five (*B. napus* cul. Windozz) and a more resistant OSR variety rated seven on the AHDB light leaf spot scale (*B. napus* cul. Nikita) (AHDB, 2022). Seeds were sown in 345-well seed trays filled with Sinclair modular seed compost. The trays were incubated in an artificially lit and glasshouse at 22-24°C with a 16:8 light:dark cycle and watered daily from above. When each plant had developed two true leaves, both leaves were harvested by cutting the petiole close to the main stem and an 8 mm diameter cork borer used to make up to 10 disks from each leaf. Disks were cut from near the edge of the leaf where there were fewer large veins, creating flat, uniform disks that would make good contact against an agar surface.

Six leaf disks from each host type were placed adaxial side upwards in a Petri dish on a 1% water-agar surface impregnated with 50ppm benzimidazole to inhibit senescence. Disks for each time/temperature and host combination were evenly spaced around the edge of a single dish approximately 1 cm from its outer edge. 5 µLs of the conidia suspension were pipetted onto the centre of each leaf disk. Petri dishes were sealed with parafilm to maintain 100% humidity during incubation.

After incubation the leaf disks were blotted dry with Whattman No.1 filter paper, then mounted on cavity slides, the adaxial surface (originally exposed to the spore droplet) facing upwards. Several drops of lactic-acid cotton-blue (Microscience Ltd) were pipetted onto the leaf surface, glass coverslips lowered onto the slide, then stained and cleared by heating to 80°C for two minutes on a hot plate. Microscopy and imaging methods of the conidia were as described earlier. The distribution of spores on the leaf surface was not uniform and spores with germtubes were more easily spotted than those that had not germinated. To avoid selection bias every spore in every image was measured.

Incubation Temperature and Duration

Artificial media experiment

A cabinet incubator (Cooling Incubators: LMS) was used to maintain the slides in complete darkness at 2.5, 5, 10, 15, 20, 22.5, 25, 27.5 or 30°C. Twelve separate slides were used for each incubation temperature, each slide was assessed once and then disposed of. The timing between assessments was staggered to create a 50°C hour interval between slide assessments resulting in an assessment every 50°C hour from 50°C hour to 650°C hour. This caused the duration of each run to vary depending on temperature. For the 30°C run the experiment was competes in 21 hours and 40 minutes whereas for run set to 2.5°C took almost eleven days. Staggering the observation times by degree hours rather than direct time periods was intended to spread observations more evenly across the germination curve at each incubation temperature.

Leaf disk experiment

A full factorial design with a limited number of temperatures and leaf wetness durations were selected for the leaf disk experiment. The results of the previous study in artificial media indicated that most *P. brassicae* conidia could germinate after 26 hours at 5°C in artificial media whilst germtube growth rate was maximum at approximately 20°C. Therefore, three incubation temperatures were used: 5, 15 and 20°C. Leaf wetness durations were also selected based on the artificial media results that were predicted to induce approximately 5, 36.8 or 95% of the maximum percentage germination given the temperature setting (A(T)).

Image Acquisition and Assessment

Artificial media experiment

After incubation slides A Leica DMC4500 camera fitted to a Leica DM2500 microscope was used to take three pictures of the hanging drop at X40 magnification with the focal plane set just below the underside of the coverslip. Each picture was taken of a different area of the hanging drop far enough away that their fields of view did not overlap to ensure that no spores were counted twice.

All images were assessed using FIJI image processing software (Schindelin et al. 2012). A total of 50 spores that were clearly visible and completely inside the field of view were chosen at random from approximately 100-300 spores visible within each field. For each spore's germtube the straight-line distance between the tip of the germtube and the point it emerged from the spore was recorded. If multiple germtubes were present the longest was selected and if a spore did not have a germtube a length of zero was recorded.

The germtube length data was transformed to create a binary variable indicating the germination status of each spore. A spore was considered to have germinated if the germtube length measurement was >3 µm. The proportion of germinated spores at each time point was calculated for each picture separately.

Leaf disk experiment

Microscopy and imaging methods of the conidia were as described for the artificial media experiment. The distribution of spores on the leaf surface was not uniform and spores with germtubes were more easily spotted than those that had not germinated. To avoid selection bias every spore in every image was measured.

Published Data Sets

Two data sets (published by Gilles et al. (2000a) and Karolewski et al. (2002) describing the maximum disease severity in relation to temperature and leaf wetness duration were collected and re-analysed using models developed from analysis of gemination and germtube development. Both data sets reported visual assessments of the percentage leaf area with sporulation over time in response to varying leaf wetness durations and incubation temperatures following inoculation by spore suspensions using handheld sprayers. Gilles et al. (2000a) reported disease severity in plants inoculated with conidia suspension with incubation temperatures of 4, 6, 8, 12, 16 and 24°C and leaf wetness durations of 6, 10, 16, 24, 48, or 72 h. Karolewski et al. 2002 used the same leaf wetness durations and a more limited set of incubation temperatures: 8, 12, 16, or 20°C but also inoculated plants with both ascospore and conidia suspension. In each case the daily assessments of the percentage

leaf area with sporulation over time were fitted with either logistic or gompertz models with parameters that explicitly represented the upper asymptote of the disease severity curve. The upper asymptotes for each combination of incubation temperature, leaf wetness duration and spore type were collected and combined into a single data set.

Field Sites

A network of field sites were established across the UK during the 2017/18 and 2018/19 growing seasons as part of the earlier mentioned CHAP SMART monitoring project. At each site four oilseed rape cultivars with AHDB resistance ratings ranging from 5 to 7 were established by direct drilling in four, six by eight-meter plots arranged edge to edge in a twelve by sixteen-meter rectangle. Crops were grown with standard fertilizer inputs, but no fungicides or insecticide applications were made. Sowing dates ranged from the 21st of August to 6th of September depending on the environmental conditions and the judgement of the site operators. The sites covered a wide range of soil types and environments across the whole of England and Wales. Most sites are situated in regions with a heavy agricultural footprint, but a few are situated in more isolated areas further away from potential sources of infection (Figure: 6). In each case the field plots were left to be infected naturally by *P. brassicae* from the local environment.

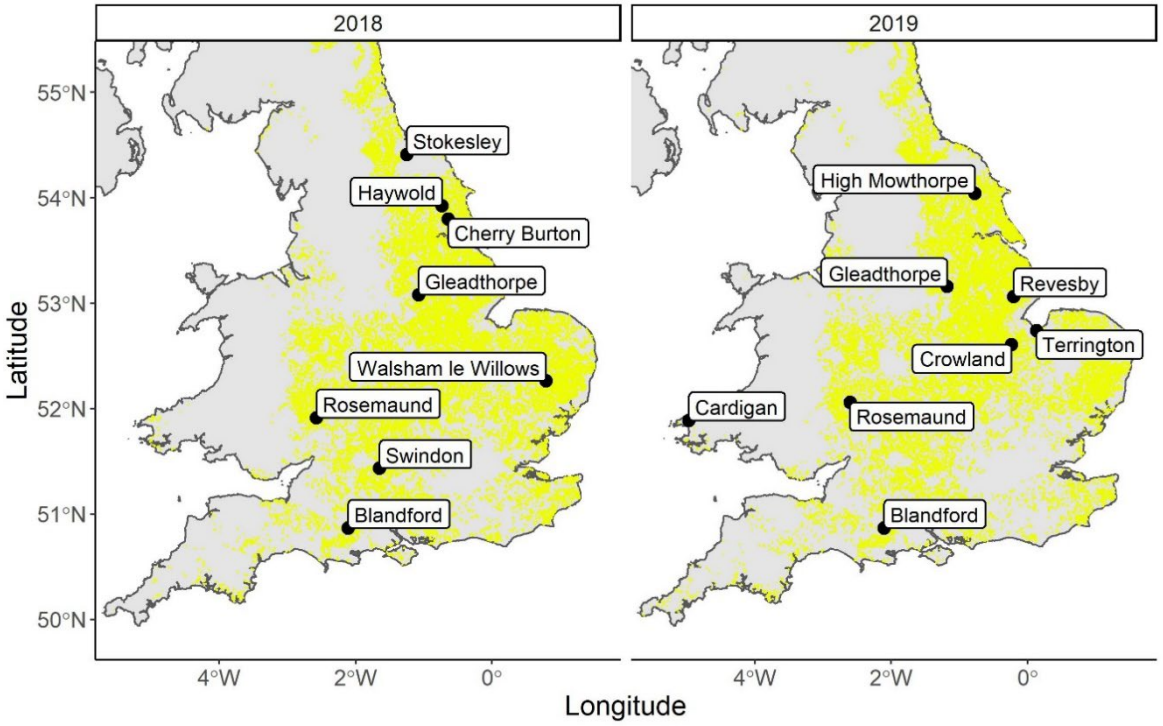

Figure 6. Locations of each field plot for which an April disease assessment was conducted for the 2017/18 (left) and 2018/19 (right) growing seasons. Yellow shading indicates the distribution of WOSR fields for each season.

Disease Monitoring

During April, when most of the field sites were at growth stage GS5, (inflorescence emergence, BSCP 2022) thirty plants from each cultivar at a subset of sixteen field-sites (Fig. 6) were selected at random and destructively assessed for the presence or absence of light leaf spot symptoms. A detailed assessment was conducted by making incidence measurements for the lower leaves, middle leaves, upper leaves and the stems of each plant. A plant was considered to be infected if any of the upper, middle or lower sections or stems contained light leaf-spot symptoms.

Weather Data

At each field site a weather station was set up within 100 m of the crop outfitted with sensors measuring temperature (°C), relative humidity (%), precipitation (mm h^{-1}), wind speed (m s^{-1}) and wind direction (°) at a 15-minute time interval. Each station was established in time for the September sowing date and data collection continued until August the following year.

Aerial Spore Monitoring

At six field sites within the 2017/18 growing season daily airborne spore samples were collected with a Burkard seven-day rotary spore trap set up within 100 m of the crop. Spore

samples over each 24h period were collected in 1.5 ml Eppendorf tubes which were sent back to Fera Science Ltd. and stored at -80°C pending molecular analysis by qPCR. At the York site all airborne ascospore samples collected between emergence and harvest were analysed. For the other five sites, only samples collected before the 30th of November were assessed to determine disease pressure at the start of the growing season - before the autumn fungicide application. The start of the spore trapping work varied between sites, in most cases sampling started in October but for the site at Rosemaund sampling did not begin until the 7th of November (Tab. 2)

Table 2: The start and end dates of analysed daily spore samples collected at York, Rosemaund, Terrington, Walsham-le-Willows, Blandford and Swindon

site id	site name	start date	end date
23	York	2017-08-29	2018-07-10
26	Walsham-le-Willows	2017-10-23	2017-11-30
34	Terrington	2017-09-25	2017-11-29
37	Swindon	2017-10-16	2017-11-30
38	Blandford	2017-10-09	2017-11-30
40	Rosemaund	2017-11-07	2017-11-30

DNA Extraction was performed by adding 150ml of soil CTAB and 20 2.3 mm zirkonica beads to each Eppendorf tube, vortexing at 1400 rpm for two minutes to liberate spores from the walls of the tube and then heating at 65°C for 10 minutes to denature potential inhibitory enzymes. Following these pre-processing steps Nuleospin Plant II spin column DNA extraction kits were used to isolate and purify the DNA from each tube following the manufacturer's instructions.

Extracted spore samples were analysed by qPCR using primers that targeted the internal transcribed spacer. The forward (**GCC GCC TAG CGC CAG T**) and reverse (**TAT ATA GTA CTC AGA CAT CAC TAA AG**) primers were made to 7.5 µmol L^{-1}. The probe was tagged with a FAM florophore and a BHQ1 quencher, to 5 µmol L^{-1} (**FAM - ATT GAG TGC CCG CCA GAG GCT - BHQ1**). qPCR reactions were prepared in duplicate with TaqMan Environmental Mastermix 2.0 following manufacturer's instructions. Analysis was performed with a quantStudio Flex 7 qPCR machine programmed to hold the samples at 50°C for 2 minutes before a 10 minute – 95°C priming step to activate the Taq-DNApolymerase. This was followed by 40 cycles of 15 seconds at 95°C and 1 minute at 60°C with a 1.6°C s^{-1} temperature gradient.

Each qPCR reaction ran alongside a negative control consisting of sterile distilled water and a set of five standards produced by extracting DNA from Eppendorf tubes spiked with 10, 100, 1000, 10,000 or 100,000 *P.brassicae* conidia. This allowed the concentration of

P.brassicae DNA in each sample to be expressed in terms of an equivalent number of conidia collected over each 24h sampling period.

Statistical Analysis

All statistical analyses were performed within the R programming environment. Linear models and statistical tests made use of the built-in stats package, non-linear models were fitted using the minpack package which provides an implementation of the Levenberg-Marquardt nonlinear least-Squares algorithm.

Germination model

Germination was modelled using a Gompertz equation ($G(t)$) modified slightly to require three parameters: *a, r, and l* which represent the upper asymptote, the maximum germination rate and the time at which the maximum germination was achieved, respectively:

Equation 1

$$\mathrm{p} = \mathrm{G(t)} = \mathrm{a}\exp\left(-\exp\left(-\left(\frac{\exp(1)\,\mathrm{r}}{\mathrm{a}}\right)(\mathrm{t}-\mathrm{l})\right)\right)$$

This model was fitted to the percentage of germinated spores (*p*) against time (*t*) for each incubation temperature separately. An ad-hoc method was developed for selecting initial parameter estimates from the data. For a, the largest observed proportion of germinated spores was used as a starting guess, the slope between the data points with percentage germination nearest the 10th and 90th percentiles was used for *r* and the *t* value of the data point with percentage germination nearest the 37th percentile for *l*. Then three additional models (*A*(*T*), *R*(*T*) & *L*(*T*)) were fitted to estimate the change in *a*, *r* and *l* against temperature (*T*), respectively:

Equation 2

$$\mathrm{p} = \mathrm{G(t|T)} = \mathrm{A(T)}\exp\left(-\exp\left(-\left(\frac{\exp(1)\,\mathrm{R(T)}}{\mathrm{A(T)}}\right)\left(\mathrm{t}-\mathrm{L(T)}\right)\right)\right)$$

Each of the three sub models required further parameters, these are denoted in the results using the convention: $b_{\mathrm{model}}^{\mathrm{parameter}}$

Growth rate model

The most probable germination time (t_{germ}) for each spore was estimated based on the distribution of germination times at each temperature ($G'(t|T)$) by:

Equation 3

$$t_{\mathrm{germ}} = \frac{1}{\int_{\mathrm{t=0}}^{\mathrm{t_{obs}}} \mathrm{G'(t|T)dt}} \cdot \int_{\mathrm{t=0}}^{\mathrm{t_{obs}}} \mathrm{t} * \mathrm{G'(t|T)dt}$$

Each spores germtube growth rate (Δg_l) was defined as a spore's measured germtube length (g_l) divided by the time difference between t_{germ} and the time the length observation was made (t_{obs}):

Equation 4

$$\Delta \mathrm{g_l} = \frac{\mathrm{g_l}}{\mathrm{t_{obs}} - t_{\mathrm{germ}}}$$

The $\Delta \mathrm{g_l}$ estimated for each spore against *T* was fitted with a log-linear model. Like the sub models used in the germination model (Equation (*)) The parameters in this model were also denoted $b_{\mathrm{model}}^{\mathrm{parameter}}$

Infection Model

Thermal time (tT) was used as a metric to evaluate the severity of infection procedures reported in the controlled environment experiments published by Gillies et al. (2000a) and Karowlewski et al. (2002). More infection events with longer thermal time were expected to increase the proportion of spores on the leaf surface capable of causing infection. The relationship between inoculum concentration and disease intensity (y) is often fitted using a restricted exponential (Madden et al 2008). Therefore, the relationship between tT and disease intensity was also fitted with a restricted exponential equation:

Equation 5

$$y = \begin{cases} \dfrac{k \cdot \left(1 - \exp\left(-b(tT - c)\right)\right),}{0,} & \text{if } tT - c \geq 0 \\ & \text{otherwise} \end{cases}$$

Where *k* is the maximum disease intensity (i.e. the visually assessed percentage of leaf area covered by conidia at the end of the experiment), *b* is the maximum rate at which disease intensity increases in response to an increase in infection severity (represented by tT) and *c* is the threshold tT required to cause infection. The disease intensities (y) reported by Karolewsiki et al (2002) and Gillies et al. (2000a) were also likely to be affected by factors other than infection severity. The temperature post infection, rater bias as well as the type of spores used to inoculate the host plants (conidia or ascospore) could all have altered the final disease intensity recorded in each experiment. To remove these potential sources of error separate *k* estimates were fitted for each incubation temperature, spore type and source study, producing eight *k* estimates for the data set reported by Karolewsiki et al (2002) and seven for Gillies et al. (2000a). This allowed a single estimate of *c* and b_r to be made when

fitting the infection model (Eqn. 5) to the whole data set; thus isolating the effects of the infection procedure from potential bias in the experimental design and variation in environmental conditions post infection.

The germination and germtube extension models were fitted to data from the artificial media experiment and subsequently refitted to the leaf disk experiment results. Analysis of variance was used to distinguish between three nested models: a 'cultivar level' model for each host type, a 'species level' model for *B. napus* and *B. oleracea* and a general model that assumed no difference between any of the host types.

Detecting infection events in the field:

A proprietary model developed at Fera Science Ltd was used to identify periods of leaf wetness at each field site based on the weather data collected between September and July. Each wetness period was further divided into periods when the temperature was within the minimum (T_{min}) and maximum (T_{max}) bounds for infection by *P.brassicae*. T_{min} and T_{max} were established based on the results of the germination and germtube growth rate models in conjunction with data in published literature. It has been established that *P. brassicae* conidia require falling water droplets to initiate splash dispersal of conidia to neighbouring plants (Pielaat et al. 2002). Therefore, infection periods that did not feature a minimum rain intensity of 2 mm h^{-1} were excluded. Of the remaining time periods an infection event was considered to have occurred if the accumulated thermal time passed the threshold for infection (c) established by fitting the infection model (Eqn. 5).

Landscape analysis of local OSR fields and ascospores

The approximate size and location of all *B. napus* fields within 10km of each site was retrieved from the UKCEH Land Cover Plus: Crops map (UKCEH, 2022) for each field plot's sowing year and harvest year. The land cover map is a procedural assessment of the crop types covering agricultural land across the UK based on satellite data collected during spring. It is provided under a non-profit license for research purposes as a geospatial data set in which each land parcel predicted to contain OSR is defined as a polygon produced from three or more x,y coordinates using the OSGB, 1936 (British National Grid) coordinate reference system. The map released for each plot's sowing year shows the nearby fields that are likely to contain debris left over from OSR crops grown the previous season, while the map released for the harvest year shows OSR fields that developed alongside each field plot. Since infected debris is thought to be an important source of inoculum for emerging oilseed rape crops (Evans et al., 2003) it is possible that the distribution of fields in the sowing year map may influence 'vertical' transmission of *P. brassicae* between growing seasons, whereas the

distribution of OSR fields in the harvest-year is more likely to be related to 'horizontal' transmission between fields in the same growing season

To estimate the relative abundance of ascospores at each site a simple spore dispersion model based on the work of Savage et al. (2011) was developed using the wind speed, wind direction and the distribution of OSR fields according to the sowing year and harvest year land cover maps (UKCEH, 2022). The data collected at each site was used to build a two dimensional ascospore distribution kernel KERN(r, θ) made from a radial ($f(r, \theta)$) component that described the probability that ascospore originating from OSR fields a given distance upwind (r) would be deposited at the centre of the field plot, and an angular component ($g(\theta)$) that described the probability density function of wind directions. Since no information was available about the disease intensity in the fields surrounding each site, each field was assumed to be equally likely to be a source of *P.brassicae* ascospores.

Results

Germination Model

For incubation temperatures at or below 27.5\degree C it was possible to fit the Gompertz model (Eqn 2) by minimising the sum of squares using the Levenberg-Marquardt non-linear least-Squares algorithm, but at 30\degree C the model could not be fitted because no germination was observed. Statistical summaries of the eight models that could be fitted indicated that the estimate for *a* (maximum percentage germination) was significant for all cases (Table 3).

Table 3. Parameter estimates for the Gompertz model (Eqn 2) fitted to the proportion of germinated spores for each incubation temperature separately. Temp is the incubation temperature; Start is the starting estimate for each parameter.

Temp.	Start	Value (95%CI)	D.F.	t-value	p-value
2.5	0.74	0.557 (0.526, 0.587)	42	35.5	<0.001
5.0	0.86	0.684 (0.658, 0.710)	63	52.0	<0.001
10.0	0.8	0.661 (0.637, 0.685)	54	53.7	<0.001
15.0	0.82	0.693 (0.648, 0.738)	60	30.2	<0.001
20.0	0.84	0.733 (0.614, 0.852)	30	12.1	<0.001
22.5	0.78	0.658 (0.627, 0.689)	45	41.8	<0.001
25.0	0.8	0.640 (0.604, 0.676)	33	34.9	<0.001
27.5	0.46	0.344 (0.315, 0.373)	30	22.9	<0.001
30.0	NA	NA	NA	NA	NA

Parameter *a* control the maximum proportion of spores that can germinate. Therefore, function $A(T)$ will model the optimal germination temperature as well as the upper and lower

temperatures between which germination is possible. These are sometimes referred to as T_{opt}, T_{min} and T_{max} or the cardinal temperatures.

The *a* parameter estimates appeared be unaffected by *T* between 5 and 22.5°C but dropped sharply as the temperature reached the upper or lower extremes. (Fig. 7). This relationship was fitted with a non-linear equation based on a quadratic linear model. The effect of *T* on *a* was fitted with an intercept and two slope parameters (b_0^a, b_1^a& b_2^a, respectively) capped by and upper threshold (b_{max}^a) that limited the maximum percentage germination that could be achieved:

Equation 6

$$A(T) = \begin{cases} b_{max}^a - \dfrac{b_{max}^a}{b_0^a + b_1^a T + b_2^a T^2}, & \text{if } T_{\text{min}} \leq T \leq T_{\text{max}} \\ 0, \text{otherwise} \end{cases}$$

Where T_{min} and T_{max} are given by:

Equation 7

$$\frac{-\mathrm{b}_1^{\mathrm{a}} \pm \sqrt{(\mathrm{b}_1^{\mathrm{a}})^2 - 4\mathrm{b}_2^{\mathrm{a}}(\mathrm{b}_0^{\mathrm{a}} - 1)}}{2\mathrm{b}_2^{\mathrm{a}}}$$

Visually, Equation 6 produced an excellent fit for the estimates of the *a* parameter (Fig. 7). However, a statistical summary revealed that only the b_{max}^a parameter was significant (Tab. 4). Unlike the original linear model, the parameters of this model do not fulfil the assumption of independence. Therefore, failure to find significance does not necessarily mean the linear parameters are not contributing to the model's fit. The 'linear' parameters (b_0^a, b_1^a& b_2^a) are most influential close to the threshold temperatures (T_{min} & T_{max}). Since most estimates of *a* were close to b_{max}^a changes in the slope at threshold temperatures had relatively little effect on the overall fit. This caused the p-value to be greater than the 0.05 critical threshold but does not necessarily mean that these parameters are not meaningful when describing the shape of the germination response curve. The estimates for T_{min} and T_{max} derived from the parameters fitted for Equation 7 were approximately 1.96 and 27.56°C respectively.

Table 4. Parameter estimates for Equation: 6 fitting the relationship between maximum percentage germination and temperature.

Parameter	Value	t-value	p-value
b^a_{max}	0.698	19.961	<0.01
b^a_0	-11.54	-0.547	0.613
b^a_1	7.22	0.753	0.494
b^a_2	-0.245	-0.321	0.488

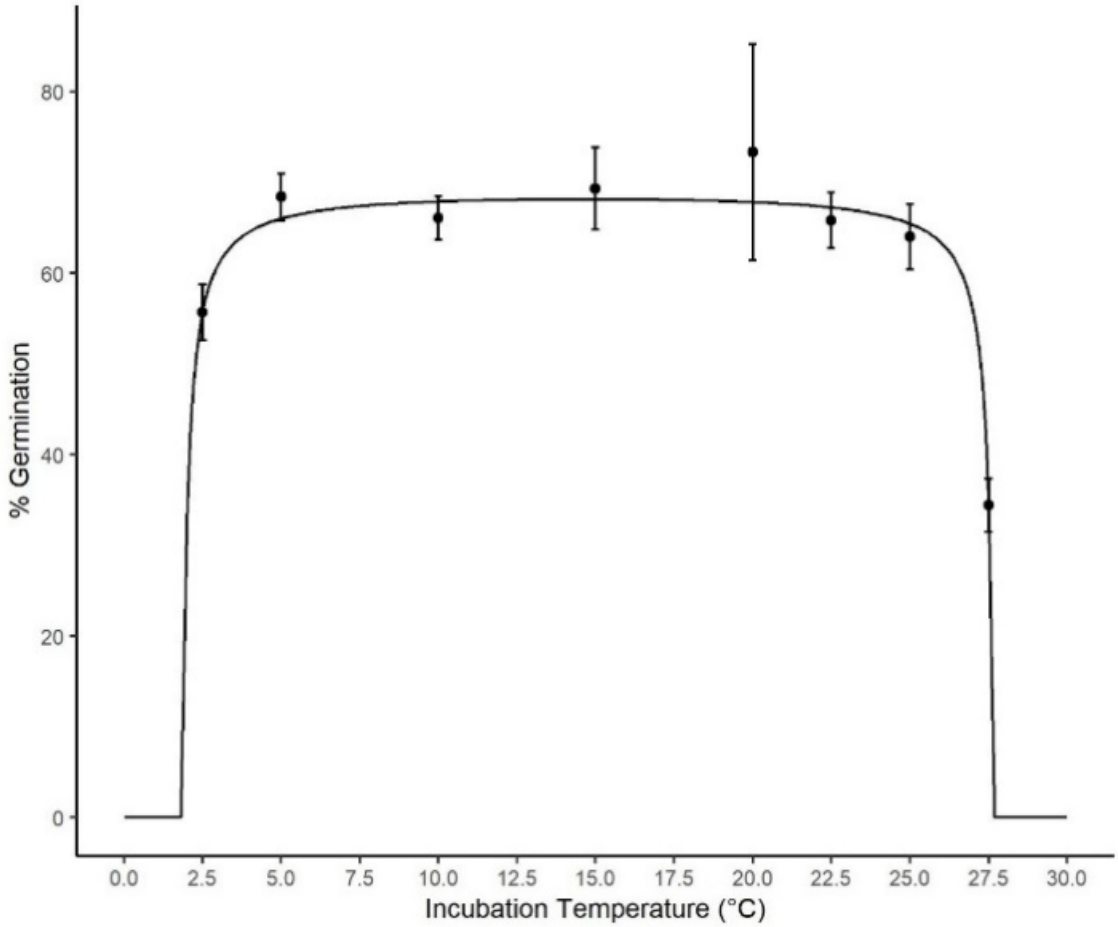

Figure 7. The maximum percentage of germination (p) against incubation temperature, black dots and error bars represent the *a* parameters of the Gompertz equation (Eqn. 2) fitted to percentage germination against time at eight different temperature settings, the solid line represents the expected maximum percentage germination given by $A(T)$ (Eqn. 6)

Germtube Growth rate Model:

When growth rate estimates were plotted against temperature, the mean growth rate increased from 0.407µm/h at 2.5°C to its steepest rate of 2.43µm/h at 20°C before dropping sharply to 0.5µm/h at 27.5°C (Fig. 8). It was found that the distribution of germtube growth rates was approximately normal for each incubation temperature but that there was close correlation between the mean germtube growth rate and the variance (Pearson's correlation = 0.947 ; t = 7.20, df = 6, p = <0.001). It appeared as though the distribution of growth rates

was tightest at low temperatures and became more dispersed as the temperature increased to 20°C, as temperature increased further the distribution contracted again but never achieved the same narrow distribution observed at the lowest temperature setting.

To model this relationship a third order linear polynomial was fitted to log transformed germtube growth rate (Δg_l) against temperature. The expected growth rate ($\widehat{\Delta g_l}$) at a given temperature could be estimated by:

Equation 8

$$\widehat{\Delta g_l} = \exp\left(b_0^{\Delta g_l} + T^1 b_1^{\Delta g_l} + T^2 b_2^{\Delta g_l} + T^3 b_3^{\Delta g_l}\right)$$

Table 5. Parameter estimates for germtube growth model (Eqn.8) showing the fitted value (Value) of each parameter (Param.); the upper and lower bounds of the 95% confidence intervals (CI95%); t-value and p-value results of a t-test for significance of each parameter on the fit of the model with 4 degrees of freedom.

Param.	Value (95% CI)			t-value	p-value
$b_0^{\Delta g_l}$	-0.918	(1.241,	-0.5951)	-7.894	0.001
$b_1^{\Delta g_l}$	-0.02089	(0.1481,	-0.1063)	-0.456	0.672
$b_2^{\Delta g_l}$	0.01581	(0.02744,	0.004182)	3.775	0.002
$b_3^{\Delta g_l}$	-0.0005290	(0.0008081,	0.007408)	-5.263	0.006

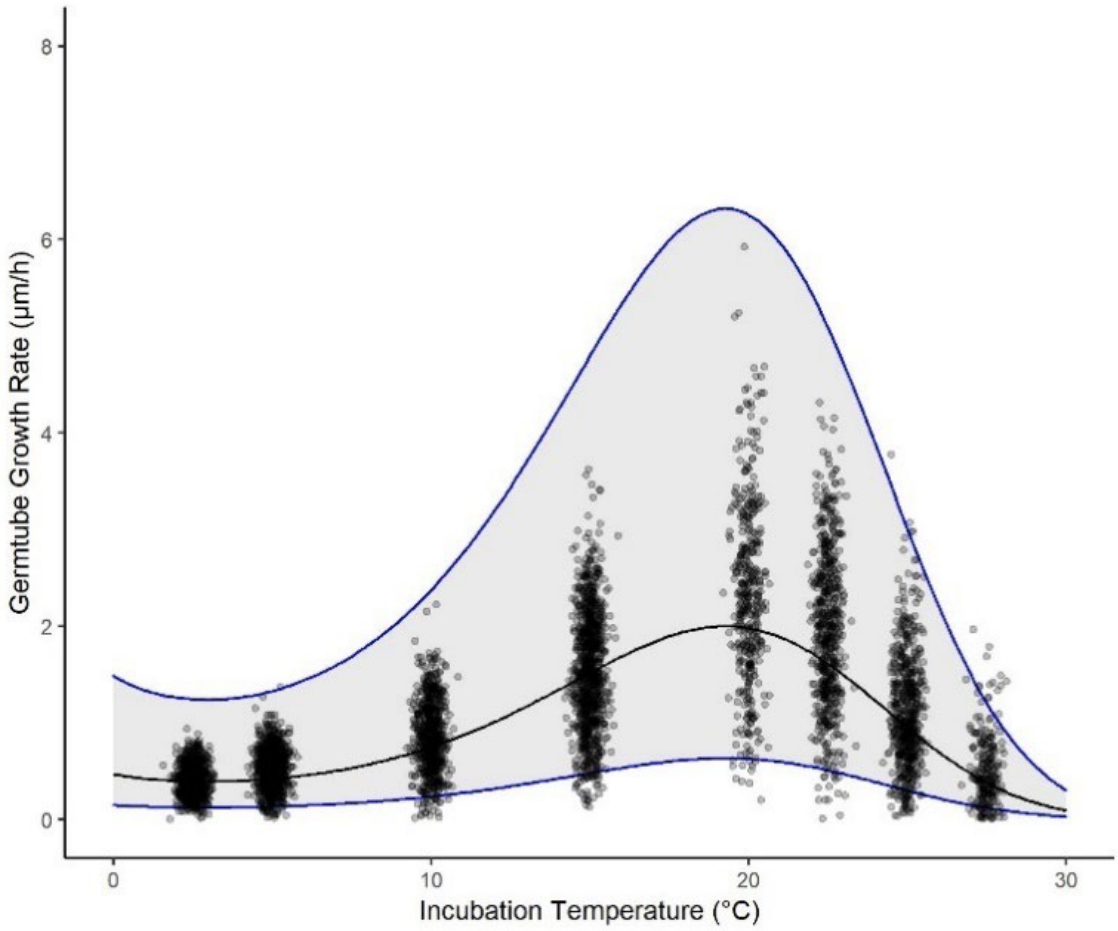

Figure 8. Growth rate of each spore estimated (Eqn 8) vs incubation temperature. The solid line represents the point-estimate of the growth rate model (Eqn 8) and the shaded area indicates the model's 95\% prediction interval.

Infection Model:

The infection model (Eqn. 5) could be fitted to all the groups in the published data sets except the final disease severities at 24°C reported by Gillies (2000a) where no visible disease symptoms developed (Tab. 6). The maximum percentage leaf area with sporulation reported in the published data varied considerably depending on incubation temperature and source study (Tab. 7). Karolewski (2002) found higher percentage leaf area values than Gillies (2000a) at 12 and 16°C and reported a decline in maximum disease severity at both 8 and 20°C with little difference between infections caused by conidia or ascospore. In contrast Gillies (2000a) did not observe a reduction in the maximum percentage leaf area with sporulation at lower temperatures (Tab 7).

Table 6. The rate (β_r)and x-intercept (c) parameters (Param.) fitted to the disease intensity data reported by (GIllies (2000) & Karolewski 2002) against thermal time during the artificially maintained leaf wetness period.

Param.	Value (95% CI)	Units	t-value	p-value
β_r	0.00621 (0.00541, 0.00711)	% h°C^{-1}	14.5	<0.001
c	90.81 (82.00, 101.00)	h°C	22.5	<0.001

The β_r and *c* parameters were both found to have relatively narrow 95% confidence intervals (Table: 6) suggesting that there is little variation in the shape of the infection curve once the variation in the maximum disease severity has been accounted for (Figure: 4). Across all permissive incubation temperatures and spore types in both studies the minimum thermal leaf wetness duration required for symptoms to develop (i.e. parameter *c*) was approximately 90.83h\degree C (Table: 6).

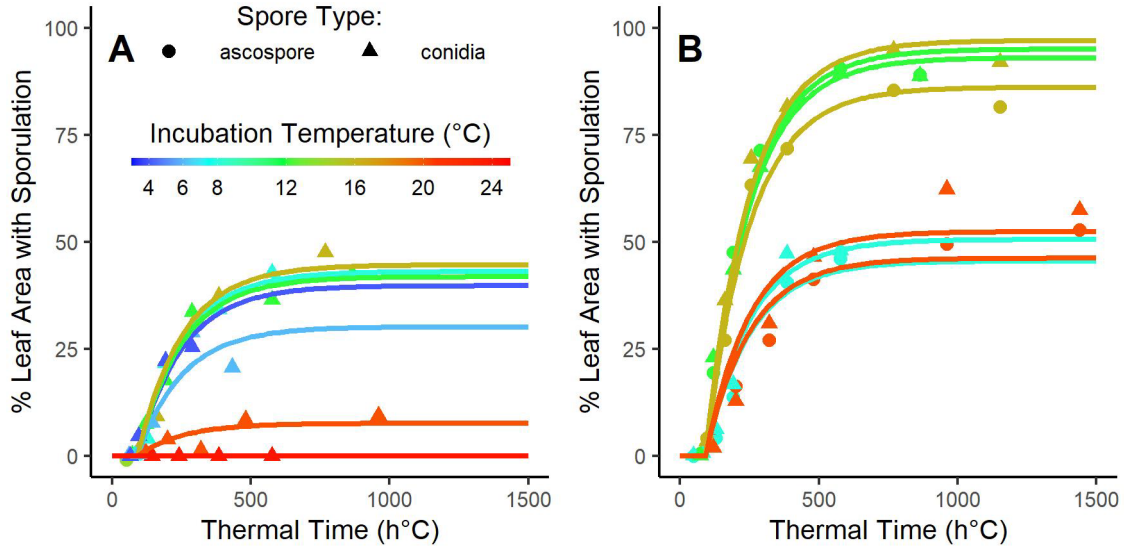

Figure 9. Percentage leaf area with sporulation in *B.napus* plants infected by *P.brassicae* reported by (A) Gilles et al. (2000a) and (B) Karolewski (2002) vs thermal time. The trend lines show a monomolecular model (Eqn 5) fitted with a single x-intercept and slope parameter but separate upper asymptotes for fifteen groups defined by the incubation temperatures, the study from which data was collected, and whether the plants were inoculated with ascospore (circles) or conidia (triangles).

Detecting Infection Events:

The site at Stokesly in the 2017/2018 growing season was abnormally dry relative to all other sites in the data set, including the weather data collected from the same site in 2018/2019 season. The plants at this site were also reported to be at a much earlier growth stage by spring than would normally be expected. It was assumed that the unusually dry weather recorded at this site was a measurement fault and that the implausibly delayed growth stage

may have been recorded erroneously. Therefore, the weather and disease data from this site in the 2017/2018 growing season was not considered in the subsequent analysis.

The leaf wetness model was applied to the temperature and relative humidity data collected at each site from the 1st of September to the 1st of July. 7,547 wet periods were detected across all twenty-six sites over the course of the monitoring period, the median duration was 11h 30min with 25 and 75 percentiles at 6.125h and 16.5h, respectively. The majority of the wet periods (88.7%) lasted less than less than 24h, but some extended much longer, the longest periods exceeding 350h of continuous wetness.

To run the infection model on data from the field sites it was necessary to establish T_{min} and T_{max}. The upper and lower temperatures for germination in artificial media were established by fitting equation 7 and found to be 1.96 and 27.56°C respectively. However, the germtube growth rate model (Eqn. 8) indicated that germtube growth rates reduce sharply as the temperature approaches 20°C (Fig. 3). The data published by Gillies (2000a) indicated that light leaf spot symptoms fail to develop at a threshold temperature between 20 and 24°C. Therefore, T_{min} was set at 1.96°C and T_{max} at 20°C. Over the sixteen growing seasons 73.0% of wet periods contained temperatures that wholly fell within this range. Of the wet periods with temperatures that fell outside T_{min} and T_{max} 21.7% contained temperatures lower than T_{min} and just 5.0% above T_{max}. The requirement for a rain intensity surpassing 2mm h^{-1} was much more discerning; only 34.2% of wet periods featured a rain intensity heavy enough to count as an infection event.

Between 33 and 68 infection events were observed between the sowing dates and the dates of the spring disease assessments in April (Tab. 7). A linear model fitted to the number of infection events between September 1st and the spring disease assessment in April was significant ($F = 10.79$, $df = 13$, $p = 0.006$); the number of infection events over the course of the growing season explaining approximately 45.35% of the variation in disease incidence in spring (Fig. 5).

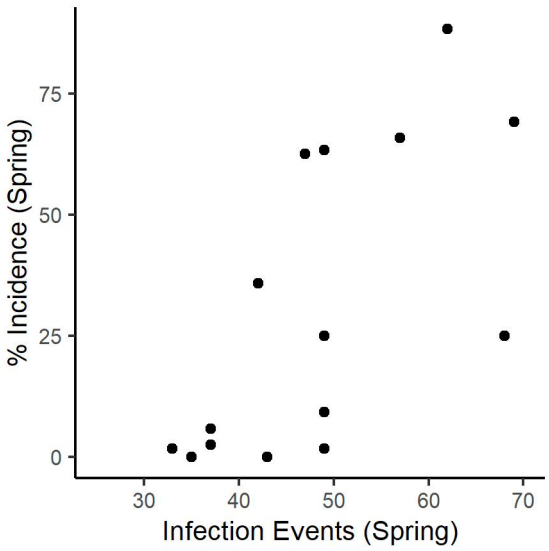

Figure 10. Percentage disease incidence from the spring assessments plotted against the number of infection events between sowing and the date the incidence observation was made.

The distribution of infection events over the growing season was fairly uniform. Suitable events appeared to be slightly more common between June and November, the distribution dipping slightly during late autumn through early spring (Fig. 11).

Table 7. The disease incidence and the number of infection events detected at each field site. Infection events are given for the period between sowing (1st September) and the initial incidence assessment in March (Reg.) and the period between sowing (1st September) and the second incidence assessment in March (Spr.)

Site Name	Harvest Year	Inf. Events	Incidence
Blandford	2018	68	0.25
Cherry Burton	2018	48	0.63
Gleadthorpe	2018	49	0.02
Haywold	2018	61	0.88
Rosemaund	2018	57	0.66
Stokesley	2018	26	0.82
Swindon	2018	68	0.69
Walsham le Willows	2018	47	0.63
Blandford	2019	46	0.25
Cardigan	2019	42	0.36
Crowland	2019	43	0.00
Gleadthorpe	2019	37	0.06
High Mowthorpe	2019	33	0.02
Revesby	2019	35	0.00
Rosemaund	2019	49	0.09
Terrington	2019	38	0.03

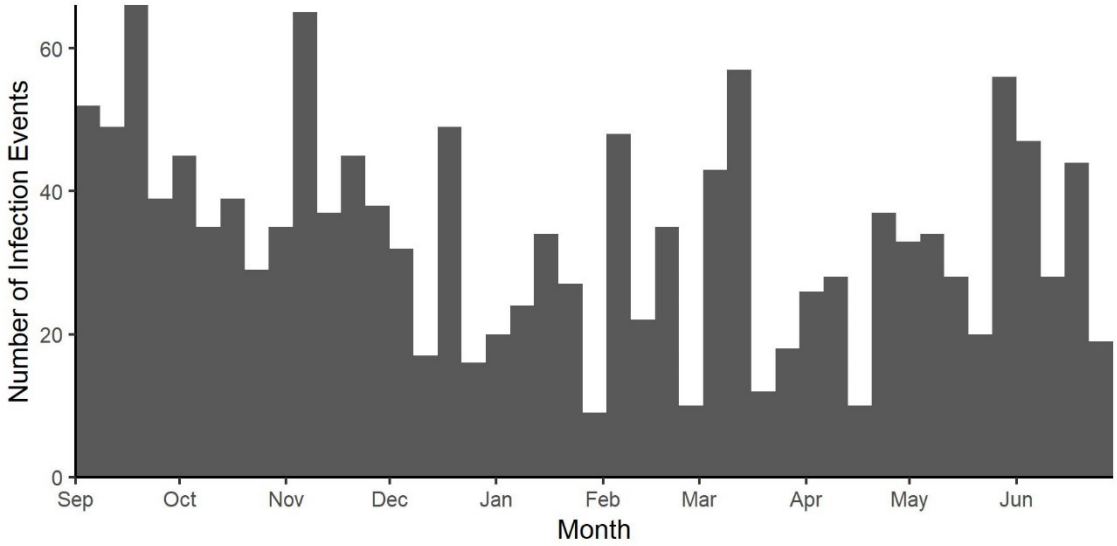

Figure 11. The distribution of infection events across all sites over the course of the WOSR growing season. The bin width is set to 7 days.

Monitoring Ascospore Concentration:

Airborne ascospore were detected at York throughout the 2017/18 monitoring period, the largest releases were observed in early Autumn soon after sampling began the with smaller episodes continuing over winter. Detection events appeared to be uniformly distributed throughout the growing season, tending towards single-day releases separated by relatively long periods with no detectable airborne spores.

Areal spores were detected at low concentrations during November at four of the six sites that were tested: York, Walsham-le-Willows, Terrington, and Rosemaund. Only Blandford and Swindon returned negative results for all sampled days (Fig. 12). Throughout the monitoring period the concentration of airborne spores was very low, the majority of positive reactions detected values that were only just above the detection threshold of the experiment, coming up between the 35th and 40th qPCR cycles. The largest concentration of *P. brassicae* DNA collected over a 24h period was equivalent to a little under twenty-five spores. In many cases the number of spores detected were below the lowest standard made for the serial dilution which contained just 10 individual conidia. Releases at York were concentrated in early autumn and spring (Fig. 13).

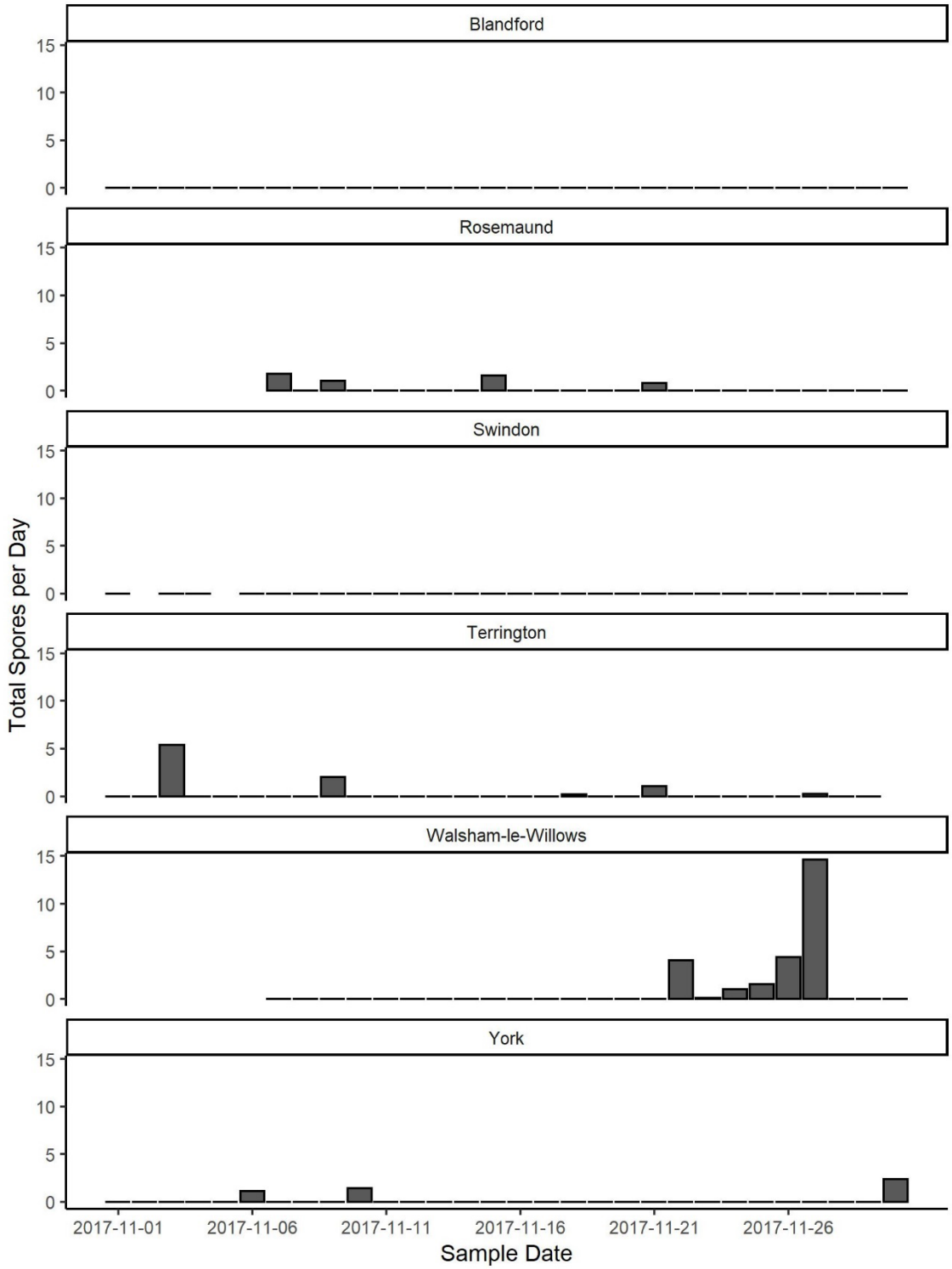

Figure 12. Number of *P.brassicae* spores detected above untreated WOSR field plots during November at Blandford, Rosemaund, Swindon, Terrington, Walsham-le-Willows and York.

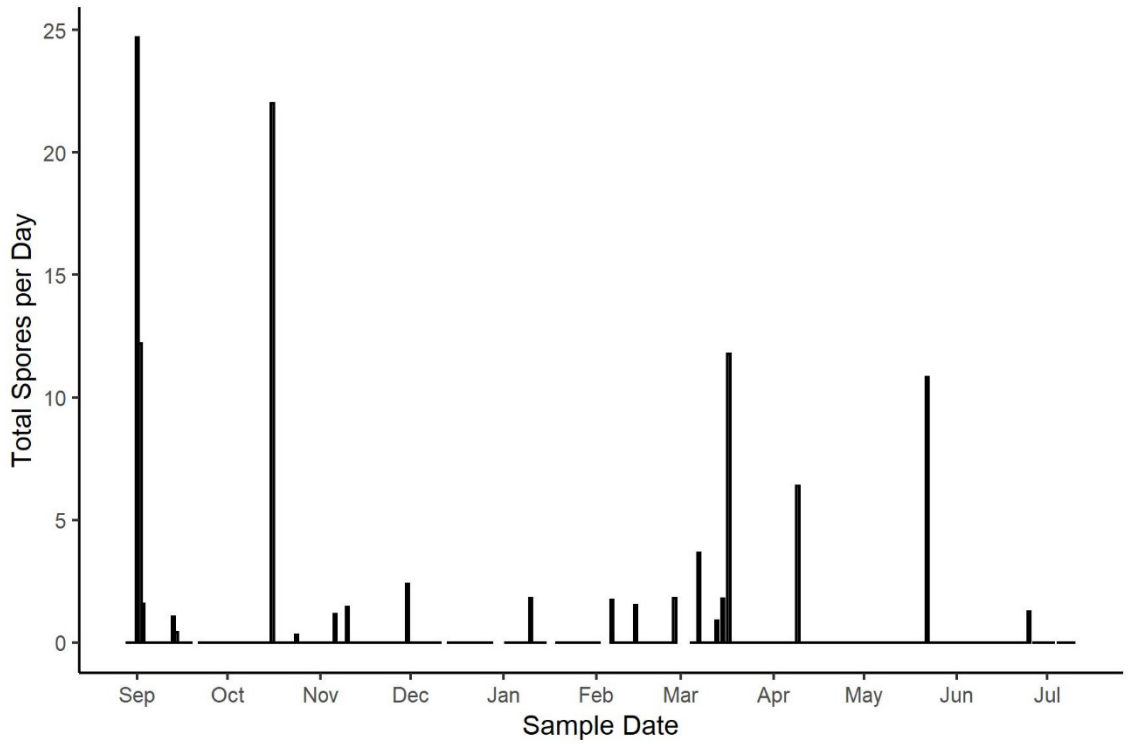

Figure 13. The number of *P. brassicae* spores detected over an untreated WOSR field plot at Fera Science Ltd between September 2017 and July 2018.

Landscape analysis of local OSR fields and ascospores

When using the sowing year OSR cropping area map there appeared to be a weak correlation between the relative ascospore density predicted by the model and the total airborne ascospores detected at each site suggesting that proximity of OSR fields harvested in July or August and airborne ascospores in November has little influence on ascospore concentration. A weak correlation was also observed between the total airborne ascospores at each site and LHA estimated using the harvest year map. Spore release height did appear to influence the strength of the relationship; the correlation was strongest when at a release height of 0.25m. However, linear models fitted to the data using the best height estimates (h) detected no significant relationship (Sowing: h = 5m, $F_{1,4}$ = 2.04, p = 0.226; Harvest: h = 0.25m, $F_{1,4}$ = 2.19, p = 0.213).

For both the sowing and harvest year OSR distribution maps very weak correlations were observed between relative ascospore density predicted by the model and incidence in the GS3 and GS5 assessments. The proximity of OSR fields around a growing site appeared to have little direct influence on the severity of the local light leaf spot epidemics. A linear model fitted to the GS3 assessments against cumulative infection events and spore dispersal based on the sowing and harvest land cover maps a was not significant ($F_{3,21}$ =1.50, p = 0.244). However, the model fitted to the GS5 disease assessments was close to the critical 0.05 threshold ($F_{3,11}$ = 3.02, p = 0.076).

Discussion

The work documented in this report revealed that the conditions under which *P. brassicae* is able to infect its hosts occur regularly throughout the growing season and that primary infection spores (ascospores) are present above crops at all times of the year. The conjunction of host, pathogen and a suitable environment at the start of the growing season implies that light leaf spot infections can occur as soon as a susceptible crop emerges from is exposed to field conditions. While the latent period of light leaf spot is known to be quite long, symptoms are thought to occur within 30 to 40 days even in sub-optimal conditions (Figueroa et al. 1995a). Thus, based on the available evidence it is reasonable to expect that infected plants should be observed much more frequently in autumn and winter than is typically the case (Evans et al., 2017). This highlights a gap in the current understanding of the light leaf spot disease cycle that hinders the development of more accurate models. It is not clear whether the apparent absence of disease early in the growing season is caused by the absence of infected plants or merely the absence of visible symptoms. This work rules out any possible explanations that suppose the conditions at the start of the growing season are not suitable for infection. Further research should focus on identifying the factors that stimulate the development of visible symptoms from latently infected tissue.

Epidemics are dynamic systems and over the past 30 to 40 years the light leaf spot epidemic has not stood still. The three components of disease: host, pathogen and environment, have all changed to greater or lesser degrees and have the potential to change further in the future. The biggest change in Brassica hosts in recent history is the rapid expansion of winter oilseed rape (WOSR). Since the mid-20th century susceptible brassica hosts have become the third most widely cultivated genus in arable regions of the UK after wheat and barley (FAOSTAT, 2012). There have been several waves of expansion, most notably a steady rise during the 80s and 90s, a plateau in the early 2000s and then a further rise during the 2010s. Recently, a rapid reduction in cropping area of WOSR can be attributed to the withdrawal of neo-nicotinoid seed treatments on which growers rely to control cabbage stem flea beetle (Ortega-Ramos et al., 2022).

Secondly, the distribution of *P. brassicae* has also changed dramatically during this time frame. Initially confined to vegetable brassica grown in the Scotland and the most northern parts of England it spread south alongside the widespread adoption of WOSR and was reported more frequently by Brassica growers in previously unaffected regions (Rawlinson et al., 1978). Reliable data for the regional incidence of *P. brassicae* began to be collected in 1987 and data collection has continued until 2021. In the 80s and 90s the severity of the annual epidemic was variable and usually only serious in Northern growing regions, but since the early 2000s it has been regularly detected in the south of England. Over time the severity

of the epidemic became less variable and currently the proportion of fields with at least one infected plant regularly exceeds 80% in most growing regions. Although this coincided with the later expansion of WOSR cropping area there is no direct evidence linking the worsening of the annual epidemic to an increase in the cropping area of susceptible hosts. However, should the observed reduction in WOSR cropping area be sustained over the next decade it may become possible to establish or rule out such a link by regressing regional WOSR cropping area against regional field level incidence data.

Third, the last component of disease, the environment, appears to have remained relatively stable in recent history. However, as global temperatures have increased since pre-industrial times the prevalence of droughts, extreme rainfall, warm winters and summer heatwaves might begin to influence the light leaf spot epidemic. Based on the AHDB light leaf spot forecast some researchers have suggested that higher summer temperatures may reduce the severity of the annual light leaf spot epidemic (Evans et al., 2010). But it is important to note that the AHDB forecast was based on a purely empirical relationship between average summer temperatures and spring disease incidence using data collected between 1987 and 1999 with no theoretical explanation of the cause of the correlation. As such it is not clear that the relationships reported by that project will still hold true following systemic changes in regional whether patterns. This report indicated that infection events, which are also correlated with epidemic severity, occur as frequently during cold wet winter months as during the warmer times of year near the start and end of the WOSR growing season. When temperatures are higher infection events can potentially be completed over shorter leaf wetness periods. Therefore, an increase in average temperatures will not necessarily reduce the number of infection events during a growing season. Infection events may be more susceptible to the availability of free water, required to cause leaf wetness, and the frequency of intense rainfall events, required for the dispersal of *P. brassicae* conidia to new host plants. Climate models have predicted that as the global climate warms the UK is likely to experience more frequent dry spells and heavy rain events (Fowler et al., 2021; Office, 2022). More detailed modelling, perhaps based on simulations on future weather data sets, are therefore recommended to predict future trends in the severity of light leaf spot epidemics.

The current AHDB forecasting system for light leaf spot is based largely on regional weather inputs collected over long time periods. Therefore, the suitability of the forecast system for growers managing individual crops is limited because its predictions are infrequent and cover a large area. The infection model developed in this report is capable of providing information about the suitability of the environment for disease development at the field level and over relatively short time spans. This will enable growers and researchers to better understand the risk of infection in relation to local weather variables. The infection model could potentially be

incorporated into current modelling systems providing an additional predictor variable where field level weather data can be provided by in-field weather stations or a gridded weather service like HadUK-grid. Alternatively, it could form the basis of a dynamic forecasting system that makes use of new or existing mechanistic models for other parts of the light leaf spot disease cycle (i.e. latency & dispersion).

Conclusions

1. The environment is suitable for infection at all times of year. There is little difference in the occurrence of infection events in summer and winter. This is likely because cooler weather in the winter is offset by longer periods of leaf wetness allowing more time for infection to occur.
2. *P. brassicae* ascospore are also present above WOSR crops throughout the year. Their distribution tends towards single day release events that sparsely distributed across the growing season. This suggests that a long period of ascospore monitoring would be required to accurately assess disease pressure at a given location. It is unlikely that this would be cost effective in a commercial setting. Since ascospore abundance observed in this project broadly agreed with abundance measured in other spore monitoring projects it can be assumed that ascospore abundance is unlikely to be rate limiting in arable regions of the UK.
3. The presence of susceptible hosts, infective material and suitable environmental conditions during at all times of year across all arable regions of the UK suggests that light leaf spot infections are likely to occur as soon as *B. oleracea* or *B. napus* plants are exposed to field conditions. Thus, more research is required to understand why light leaf symptoms are not observed in either crop type until much later in their respective growing seasons. It may be that the latent period is has a more complicated relationship with time and temperature than was previously thought, perhaps requiring a wetter or colder environmental conditions or for the host to reach a certain growth stage to stimulate conidia production and other visible symptoms. Alternatively, it may be that the relatively low concentration of *P. brassicae* ascospore causes primary infection events to be relatively rare, thus the incidence of infected plants with visible symptoms remains below the detection threshold until much later in the growing season.
4. A reasonably strong correlation was observed between the number of infection events between sowing and April and visually assessed disease incidence in WOSR plants in Spring. Since infection events are based on a more theoretical relationship between

field level weather data and the *P. brassicae* disease cycle this variable is likely to be more robust to future changes in weather patterns. The infection model could potentially be incorporated into the current AHDB light leaf spot forecast as an additional field level variable. Doing so would require that field level weather be supplied for individual fields, either via the HadUK-girid supplied by the met office or from weather stations placed in or around the field of interest.

Knowledge and Technology Transfer

- BCSP conference 2018 – Poster
- Fera Conference 2018 - Poster
- AHDB conference_2018 - Presentation
- Fera Conference 2019 – Presentation
- Snes Conference 2019 - Poster
- AHDB conference 2020 - Poster
- Fera Conference 2020 - Presentation
- IAFRI Conference 2020 – Poster
- AHDB conference 2021 - Presentation

References

AHDB (2022) Light Leaf Spot Forecast. URL: https://ahdb.org.uk/light-leaf-spot-forecast. (Visited: 2022-05-27)

Anonymous (2019) *Alert to light leaf spot risk.* URL: https://www.syngenta.co.uk/news/agronomy-issues/alert-light-leaf-spot-risk. (visited: 01/06/2021)

Ashby A M (1997) A molecular view through the looking glass: the Pyrenopeziza brassicae-Brassica interaction. *Advances in Botanical Research* 24. pp. 31-70.

Ashby A M (2000) Biotrophy and the Cytokinin Conundrum. *Physiological and Molecular Plant Pathology* 57.4. pp. 147-158.

Behrends R, Dillon L K, Fleming S D, Stirewalt R E K (2020) Diseases of Vegetable Brassicas. URL: https://www.researchgate.net/publication/341726937_Diseases_of_Vegetable_Brassicas. (Visited 24-05-2022)

Boys E F, Roques S, Ashby A, Evans N, Latunde-Dada A, Thomas J, West J, Fitt, B D L (2007) Resistance to Infection by Stealth: *Brassica napus* (Winter Oil Seed Rape) and *Pyrenopeziza brassicae* (Light Leaf Spot). *Eur J Plant Pathol* 118.4. Number: 4, p. 307.

ISSN: 1573-8469. DOI: 10.1007/s10656-007-9141-9. URL https://doi.org/10.1007/s10656-007-9141-9

Boys E F, Roques S E, West J S, Werner C P, King G J, Dyer P S, Fitt B D L (2012) Effects of R Gene-Mediated Resistance in *Brassica napus* (Oilseed Rape) on Asexual and Sexual Sporulation of *Pyrenopeziza brassicae* (Light Leaf Spot). *Plant Pathology* 61.3. pp. 543-554.

Davies K A, De Lorono I, Foster S J, Li D, Johnstone K, Ashby A M (2000) Evidence for a Role of Cutinase in Pathogenicity of *Pyrenopeziza brassicae* on Brassicas. *Physiological and Molecular Plant Pathology* 57.2. pp. 63-75

Evans N, Baierl A, Brain P, Welham S J, Fitt B D L (2003) Spatial Aspects of light Leaf Spot (*Pyrenopeziza brassicae*) Epidemic Development on Winter Oilseed Rape (*Brassica napus*) in the United Kingdom. *Phytopathology 93.6.* Number: 6, pp. 657-665. ISSN: 0031-949X. DOI: 10.1094/PHYTO.2003.93.6.657. URL: https//apsjournals.apsnet.org/doi/abs/10.1094/PHYTO.2003.93.6.657

Evans N, Ritchiem F, West J, Havis N, Matthewman C, Maguire K (2017) Investigating Components of the Oilseed Rape Light Leaf Sport Epidemic Responsible for Increased Yield Loss to the UK Arable Industry. *Tech. Rep.* PR587. AHDB Cereals & Oilseeds and Bayer CropScience.

Evans N, Butterworth M H, Baierl A, Semenov M A, West J S, Barnes A, Moran D, Fitt BDL (2010) The impact of climate change on disease constraints on production of oilseed rape. *Food Security* 2.2. pp. 143 - 156

FAOSTAT (2022) Food and Agriculture Data. URL: https://www.fao.org/faostat/en/#home. (Visited: 2022-05-28)

Figueroa L, Shaw M W, Fitt B D L, McCartney H A, Welham, S J (1994) Effects of Previous cropping and fungicide timing on the development of light leaf spot (Pyrenopeziza brassicae), seed yield and quality of winter oilseed rape (Brassica napus). *Annals of Applied Biology* 124.2. pp. 221-239.

Figueroa L, Fitt B D L, Welham S J, Shaw M W, McCartney H A (1995a) Early Development of Light Leaf Spot (*Pyrenopeziza brassicae*) on Winter Oilseed Rape (*Brassica napus*) in Relation to Temperature and Leaf Wetness. *Plant Pathology* 44.4. pp 641-654.

Figueroa L, Fitt B D L, Shaw M W, McCartney H A, Welham, S J (1995b) Effects of Temperature on the Development of Light Leaf Spot (*Pyrenopeziza brassicae*) on Oilseed Rape (*Brassica napus*). *Plant Pathology* 44.1. pp. 51-62

Fitt B D L, and Doughty K J, Gladders P, Steed J M, Sutherland K G (1998a) Diagnosis of Light Leaf Spot (*Pyrenopeziza brassicae*) on Winter Oilseed Rape (*Brassica napus*) in the UK. *Annals of Applied Biology* 133.2. pp 155-166.

Gilles T, Fitt B D L, Kennedy R, Welham S J, Jeger, M J (2000a) Effects of Temperature and Wetness Duration on Conidial Infection, Latent Period and Asexual Sporulation of *Pyrenopeziza brassicae* on Leaves of Oilseed Rape. *Plant Pathology* 49.4. pp. 498-508.

Gilles T, Evans N, Fitt B D L, Jeger M J (2000b) Epidemiology in Relation to Methods for Forecasting Light Leaf Spot (*Pyrenopeziza brassicae*) Severity on Winter Oilseed Rape (*Brassica napus*) in the UK. *Eur J Plant Pathol* 106.7. pp. 593-605.

Gilles T, Fitt B D L, Jeger M J (2001a) Effects of Environmental Factors on Development of *Pyrenopeziza brassicae* (Light Leaf Spot) Apothecia on Oilseed Rape Debris. *Phytopathology* 91.4. pp 392-398.

Gilles T, Fitt B D L, Welham S J, Evans N, Steed J M, Jeger M J (2001b) Modelling the Effects of Temperature and Wetness Duration on Development of Light Leaf Spot on Oilseed Rape Leaves Inoculated with *Pyrenopeziza brassicae* Conidia. *Plant Pathology* 50.1. pp 42-52

Gilles T, Fitt B D L, McCartney H A, Papastamati K, Steed J M (2001c) The Roles of Ascospores and Conidia of *Pyrenopeziza brassicae* in Light Leaf Spot Epidemics on Winter Oilseed Rape (*Brassica napus*) in the UK. *Annals of Applied Biology* 138.2. pp 141-152.

Kang W S, Hong S S, Han Y K, Kim K R, Kim S G, Park E W (2010) A Web-Based Information System for Plant Disease Forecast Based on Weather Data at High Spatial Resolution. *The Plant Pathology Journal* 26.1. pp. 37-48.

Karandeni Dewage C S, Qi A, Stotz H U, Huang Y, Fitt B D L (2021) Interactions in the *Brassica napus--Pyrenopeziza brassicae* Pathosystem and Sources of Resistance to *P. brassicae* (Light Leaf Spot). *Plant Pathology* 70.9. pp. 2104-2114

Karandeni Dewage C S, Cools K, Stotz H, Qi A, Huang Y, Wells R, Fitt B D L (2022) QTL Mapping for Resistance Against *Pyrenopeziza brassicae* Derived from a *Brassica napus* Secondary Gene Pool. *Frontiers in Plant Science*. DOI: https://doi.org/10.3389/fpls.2022.786189

Karolewski Z, Evans N, Fitt B D L, Todd A D, Baierl A (2002) Sporulation of *Pyrenopeziza brassicae* (Light Leaf Spot) on Oilseed Rape (*Brassica napus*) Leaves Inoculated with Ascospores or Conidia at Different Temperatures and Wetness Durations. *Plant Pathology* 51.5. pp 654-665. *Frontiers in Plant Science.*

Karolewski Z, Evans N, Fitt B D L, Baierl A, Todd A D, Foster S J (2004) Comparative Epidemiology of *Pyrenopeziza brassicae* (Light Leaf Spot) Ascospores and Conidia from Polish and UK Populations. *Plant Pathology* 53.1. pp 29-37.

Karolewski Z, Fitt B D L, Latunde-Dada A O, Foster S J, Todd A D, Downes K, Evans N (2006) Visual and PCR Assessment of Light Leaf Spot (*Pyrenopeziza brassicae*) on Winter Oilseed Rape (*Brassica napus*) Cultivars. *Plant Pathology* 55.3. pp 29-37.

Karolewski Z (2010) Development of light leaf spot (Pyrenpoeziza brassicae) on brassicas. *Phytopathologica* 55, pp. 13-20

Karolewski Z, Kaczmarek J, Jedryczka M, Cools H J, Fraaije B A, Lucas J A, Latunde-Dada A O (2012) Detection and Quantification of Airborne Inoculum of *Pyrenopeziza brassicae* in Polish and UK Winter Oilseed Rape Crops by Real-Time qPCR Assays. *Grana* 51.4 pp 270-279.

Li D, Ashby A M, Johnstone K (2003) Molecular Evidence that the Extracellular Cutinase Pbc1 Is Required for Pathogenicity of Pyrenopeziza brassicae on Oilseed Rape. *MPMI* 16.6. pp. 545-552

Maddock S E, Ingram D S (1981) Studies of survival and longevity of the light leaf spot pathogen of brassicas, Pyrenopeziza brassicae. *Transactions of the British Mycological Society* 77.11. pp. 153-159

Margarey R D, Sutton T B and Thayer C L (2005) A simple generic infection model for foliar fungal plant pathogens. *Phytopathology* 95:1, pp 92-100.

McCartney H A, Lacey M E, Rawlinson C J (1986) Dispersal of *Pyrenopeziza brassicae* spores from an Oilseed Rape Crop. *The Journal of Agricultural Science* 107.2, pp. 299-305.

McCartney H A, Lacey M E (1989) The Production and Dispersal of Ascospores of *Pyrenopeziza brassicae* in Oilseed Rape Crops. *Aspects of Applied Biology* 23. Pp. 401-408.

Ortega-Ramos P A, Cook S M, Mauchline A L (2022) How Contradictory EU Policies Led to the Development of a Pest: The Story of Oilseed Rape and the Cabbage Stem Flea Beetle. *GCB Bioenergy* 14.3. pp 258 – 266.

Papastamati K, Van Den Bosch F, Welham S J, Fitt B D L, Evans N, Steed J M (2002) Modelling the Daily Progress of Light Leaf Spot Epidemics on Winter Oilseed Rape (*Brassica napus*), in Relation to *Pyrenopeziza brassicae* Inoculum Concentrations and Weather Factors. *Ecological Modelling* 148.2. pp 169-189

Pielaat A, Van Den Bosch F, Fitt B D L, Jeger M J (2002) Simulation of Vertical Spread of Plant Diseases in a Crop Canopy by Stem Extension and Splash Dispersal. *Ecological Modelling* 151.2-3. Pp. 195-212.

Rawlinson C J, Sutton B C and Muthyalu G (1978) Taxonomy and biology of Pyrenopeziza brassicae sp.nov (Cylindrosporium concentricum), a pathogen of winter oilseed rape (Brassica napus spp. Oleifera. *Transactions of the British Mycological Society* 71.3. Number: 3. pp 425-439. ISSN: 00071536. DOI 10.1016/S0007-153678800709

Savage, D, M J Barbetti, W J MacLeod, MU Salam, and M Renton (2011). Can mechanistically pararneterised, anisotropic dispersal kernels provide a reliable estimate of wind-assisted dispersal? *Ecological Modelling* 222.10, pp. 1673-1682.

Sharp C (2022) Brassica Alert. URL: httpe://www.syngenta.co.uk/brassica-alert (visited on 27/05/2022)

Schindelin J, Arganda-Carreras I, Frise E, Kaynig V, Longair M, Pietzsch T, Preibisch S, Rueden C, Saalfeld S, Schmid B, Tinevez J, White D J, Hartenstein V, Eliceiri K, Tomancak P, Cardona A (2012) Fiji: an Open-Source Platform for Biological-Image Analysis. *Nature Methods* 9.7. pp 676-682

Thayer, C L (2006) Plant Disease Forecasting and Model Validation: Classic and Modern Approaches. NC State University Libraries - Masters Thesis. URL: http://www.lib.ncsu.edu/resolver/1840.16/2002

UKCEH (2022). Land Cover Plus: Crops. https://www.ceh.ac.uk/services/ceh-land-cover-plus-crops-2015#case (visited on 05/30/2022).

UKMO (2022) HadUK-Grid: Gridded Climate Observations for the UK. URL: https://www.metoffice.gov.uk/research/climate/maps-and-data/data/haduk-grid/datasets. (Visited: 2022-05-30)

de Vallavieille-Pope, C and Huber, L and Leconte, M and Goyeau, H (1995) Comparative Effects of Temperature and Interrupted Wet Periods on Germination, Penetration, and Infection of *Puccinia recondita* f. sp. tritici and *P. striiformis* on Wheat Seedlings. *Phytopathology* 85.4. pp. 409-415.

Welham S J, Turner J A, Gladders P, Fitt B D L, Evans N, Baierl A (2004) Predicting Light Leaf Spot (*Pyrenopeziza brassicae*) Risk on Winter Oilseed Rape (*Brassica napus*) in England and Wales, Using Survey, Weather and Crop Information. *Plant Pathology* 53.6. pp. 713-724

